LASERLAB-EUROPE

The Integrated Initiative of European Laser Research Infrastructures III

Grant Agreement number: 284464

Work package WP33
"European Research Objectives on Lasers for Industry, Technology and Energy (EURO-LITE)"

Deliverable D33.30
"Final report on laser characteristics improvements for fs/as pulse generation"

Lead Beneficiary: GSI-HIJ

Due date: 11/30/2015

Date of delivery: 11/19/2015

Project webpage: www.laserlab-europe.eu

Deliverable Nature	
R = Report, P = Prototype, D = Demonstrator, O = Other	R
Dissemination Level	
PU = Public	PU
PP = Restricted to other programme participants (incl. the Commission Services)	
RE = Restricted to a group specified by the consortium (incl. the Commission Services)	
CO = Confidential, only for members of the consortium (incl. the Commission Services)	

A. Abstract / Executive Summary

The LASERLAB partners involved in EUROLITE have developed advanced, innovative laser technology and set-ups for the generation of high-energy attosecond pulses. Their investigations covered the laser driver, the optimisation of the High Harmonic Generation (HHG) process and the stabilisation and characterisation of the Carrier Envelope Phase (CEP).

Complementary approaches have been followed for the laser driver. LOA developed a high contrast TiS laser associated with an original post-compression set-up to produce 3,5 mJ, sub-4 fs pulses at 800 nm. MPQ and ICFO focused on mid-infrared sources based on parametric amplification. The set-up developed at MPQ relies on optical parametric chirped pulse amplification (OPCPA) of infrared pulses at 2.1 µm whereas ICFO implemented an Optical Parametric Amplifier (OPA) that generates sub-2-cycle pulses at 1850 nm. The ICFO set-up allowed producing isolated attosecond soft X-ray pulses in the water window spectral range for applications in life science. CELIA investigated the potential of Fiber Chirped Pulse Amplification (FCPA) to get laser operation at very high rep rate (100 kHz) and high average power. The CELIA laser demonstrated 50W power at 1030 nm and was successfully used to generate HHG in gases up to the 29th harmonic with microjoule energy.

Optimisation of the HHG process has also been investigated. HIJ focused on the optimisation of surface harmonic generation under different contrast configurations and with structures targets. Using an optimised version of the interferometric polarisation gating scheme, FORTH achieved generation of XUV super-continua confined in sub-fs pulses whose high energy was verified through the first XUV-pump-XUV-probe studies of 1fs scale atomic and molecular dynamics.

In addition, different schemes for CEP stabilisation and characterisation were studied. SLIC implemented different stabilisations setups based on Electro-optic phase shifters that were optimised either for larger correction bandwidth and/or to achieve isochronous stabilisation. HIJ and MPQ demonstrated single shot CEP characterisation using an ATI (Above Threshold Ionisation) phasemeter on a multi-Terawatt laser and Electro Optic Sampling respectively. Finally, LENS developed setups in the mid-IR for ultra-sensitive spectroscopic applications of atmospheric and astrophysical interest.

B. Deliverable Report

1   Introduction

The advent of utltrafast lasers made it possible to use light as a powerful tool for exploring the dynamics of nuclear and electronic wavepackets, which are among the fastest motions in matter. Since the time scale for the electron dynamics in matter is femtoseconds or less, attosecond light pulses are needed. These ultimately short pulses are produced as secondary sources, from the nonlinear conversion of the driving IR-vis-UV femtosecond laser pulses into the extreme-UV and X-ray range through High Harmonic Generation (HHG).

For such short pulses, full control of the action of the electric field on matter at the optical cycle scale is necessary. This implies a perfect reproducibility of the temporal shape of the light pulse through Carrier Envelope Phase (CEP) control. These requirements imply driving lasers in the IR-vis-UV range that can deliver ultrashort, high energy pulses with CEP control, preferably at high repetition rate (1-100 kHz). Nowadays, most of the systems used for femtosecond and attosecond science are based on Titanium-Sapphire (TiS) CPA lasers. In

parallel, laser research investigates Optical Parametric Amplification (OPA) and of Optical Parametric Chirped Pulse Amplification (OPCPA), in particular when ultimately short pulse duration (<10fs), longer wavelength (1-4µm), very high repetition rate (>10kHz) or self CEP stabilisation are required.

EUROLITE, through the Objective 3 aims at contributing to the development of these ultrafast laser drivers with a special focus on higher pulse energies, increased repetition rates, broader wavelength coverage and optimised Carrier-Envelope Phase (CEP) stabilisation. Optimising the efficiency of HHG is also an important objective towards attosecond pulse generation. This report summarises the work carried out from June 2012 to November 2015 by the 8 Laserlab partners involved in this activity.

2　Objectives

The work carried out within the Objective 3 of EUROLITE had 3 main objectives.

The first objective was to develop advanced driving lasers and post-compression set-ups for the generation of high-energy attosecond pulses. Different schemes were tested. LOA and HIJ had the task to develop lasers based on Titanium-Sapphire (TiS) featuring high contrast at high repetition rate. ICFO and MPQ tasks were to develop parametric amplifiers in the Mid-IR since the scaling of the high-harmonic generation (HHG) process that lays behind attosecond pulse generation favours longer wavelengths to reach higher energies. ICFO focused on an Optical Parametric Amplifier (OPA) operating at 1.85 µm whereas MPQ opted for an OPCPA (Optical Parametric Chirped Pulse Amplifier) emitting at 2.1µm and pumped by a picosecond Yb:YAG thin disk amplifier. Finally, CELIA's task was to investigate the potential of Fiber Chired Pulse Amplification (FCPA) to generate short pulses at high repetition rate (100 kHz) with high energy.

The second objective was to produce high energy, large bandwidth femto/atto XUV pulses. HIJ's task focused on finding the best conditions in terms of temporal contrast to maximise the efficiency of the HHG process on solid targets and therefore optimise the XUV pulse energy. ICFO optimised a set-up to push the XUV pulse wavelength down to the water window while CELIA scheme was optimised for high repletion rate low energy driving laser.. FORTH and HIJ tasks were also to implement and optimise the interferometric temporal gating scheme that allows confining the attosecond emission within a half optical cycle even when using many cycle high peak power lasers. MPQ's tasks include the implementation of complete attosecond beamlines. Finally, specific optics for attosecond pulses were also tested at HIJ.

The third objective dealt with the optimisation of Carrier Envelope Phase (CEP) control through new stabilisation or characterisation schemes. The concept of the Electro-Optic phase shifter was investigated by SLIC with monolithic or isochronous set-ups. HIJ and MPQ focused on CEP single shot measurement using by an ATI (Above Threshold ionisation) phasemeter and Electro-optic sampling respectively.

In addition, LENS had the task of investigating the use of CEP stabilised sources for extending the frequency-comb advantages to the Mid-IR. Advanced lasers and set-ups were developed that allow for ultra-sensitive detection and monitoring of molecules of atmospheric and astrophysical interest.

3   Work performed / results / description

3.1   Driving lasers and post-compression set-ups for the generation of attosecond pulses

Development of ultrafast laser drivers specifically optimised for attosecond pulses generation has been carried out at LOA, ICFO, MPQ, and CELIA. Each partner investigated a different technics: high contrast Titanium-Sapphire lasers at LOA and HIJ, Optical Parametric Amplification in the mid-Infrared at ICFO, Chirped Pulse Optical Parametric Amplification in the mid-Infrared at MPQ and high repetition rate Fiber Chirped Pulse Amplification at CELIA. In most cases, these lasers were associated with post-compression set-ups to further decrease their pulse duration down to a few optical cycles.

3.1.1   OPCPA and attosecond beamline developments (MPQ)

⊕   Objectives

The work that has taken place at MPQ aimed at using and extending the capabilities of optical chirped pulse parametric amplification (OPCPA) systems pumped by Yb:YAG thin disk lasers to produce carrier-envelope-phase-stable few-cycle pulses at 2.1 μm central wavelength with mJ-scale energy at multi-kHz repetition rates. In order to produce a laser system applicable to detailed scientific work, significant advances were necessary in both the reliability of the underlying laser technology and the pulse diagnostics. The MPQ team has improved both aspects of the system described in [1] such that it will shortly become a workhorse laser driving an attosecond beamline that was recently implemented and is described in section 3.2.5.

⊕   Laser system improvements

The laser system used is based upon the Yb:YAG thin-disk regenerative amplifier reported by Metzger *et al.* [2]. Additional second-harmonic frequency resolved optical gating (SHG-FROG) measurements of the laser pulse showed recently that the B-integral (acquired nonlinear phase) was high enough that there were significant day-to-day changes in the pump pulse characteristics, which harmed the reproducibility of the OPCPA, lengthened the pulse and significantly reduced the stability of the peak power.
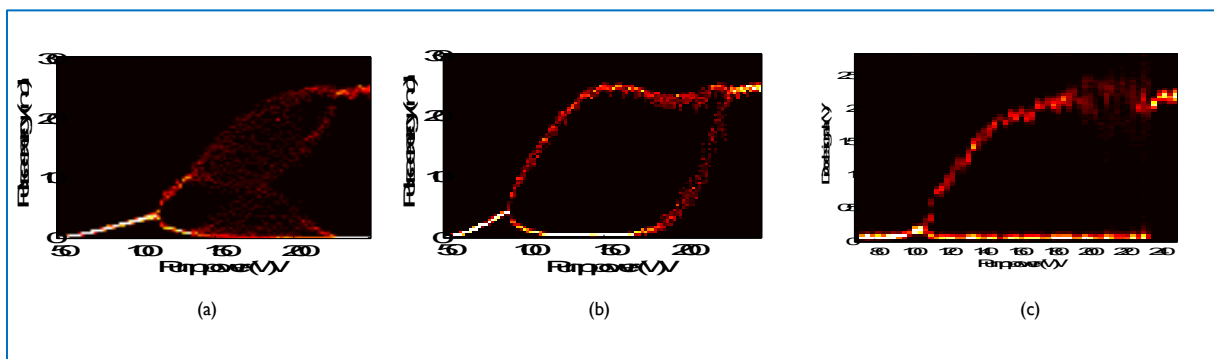

Figure 1. amplification dynamics in CW-pumped thin-disk amplifier. (a) simulation of operation with 6 kHz Pockels cell frequency, resulting in period doubling (operation at 3 kHz) with pump power above 225 W, and chaotic behavior below. (b) simulation of operation with 3 kHz Pockels cell frequency, also resulting in 3 kHz operation, and no chaotic behavior at lower pump intensities (only bifurcation). (c) experimental observation of the stable cavity dynamics predicted in (b), with a one-to-one correspondence between injected and amplified pulses above 230 W pump power, beneficial since the OPCPA utilized optical synchronization with a seed source operating at 3 kHz. Adapted from [3].

This led the MPQ group to model and improve the pulse dynamics inside of the cavity through four main improvements: additional pre-amplification in fibre amplifiers provided by the group of Jens Limpert, a strategy of using a minimal number of round trips through the cavity, change in the timing properties such that the laser operates with a Pockels cell frequency of 3 kHz with every pulse amplified rather than the period doubling mode used in [1] and a re-designed cavity. The change in amplification dynamics is illustrated in Figure 1, showing the elimination of chaotic amplification. The improvement of pulse quality and reduction of B-integral resulting from the higher seed level is illustrated in Figure 2. The improved cavity design is shown in Figure 3.
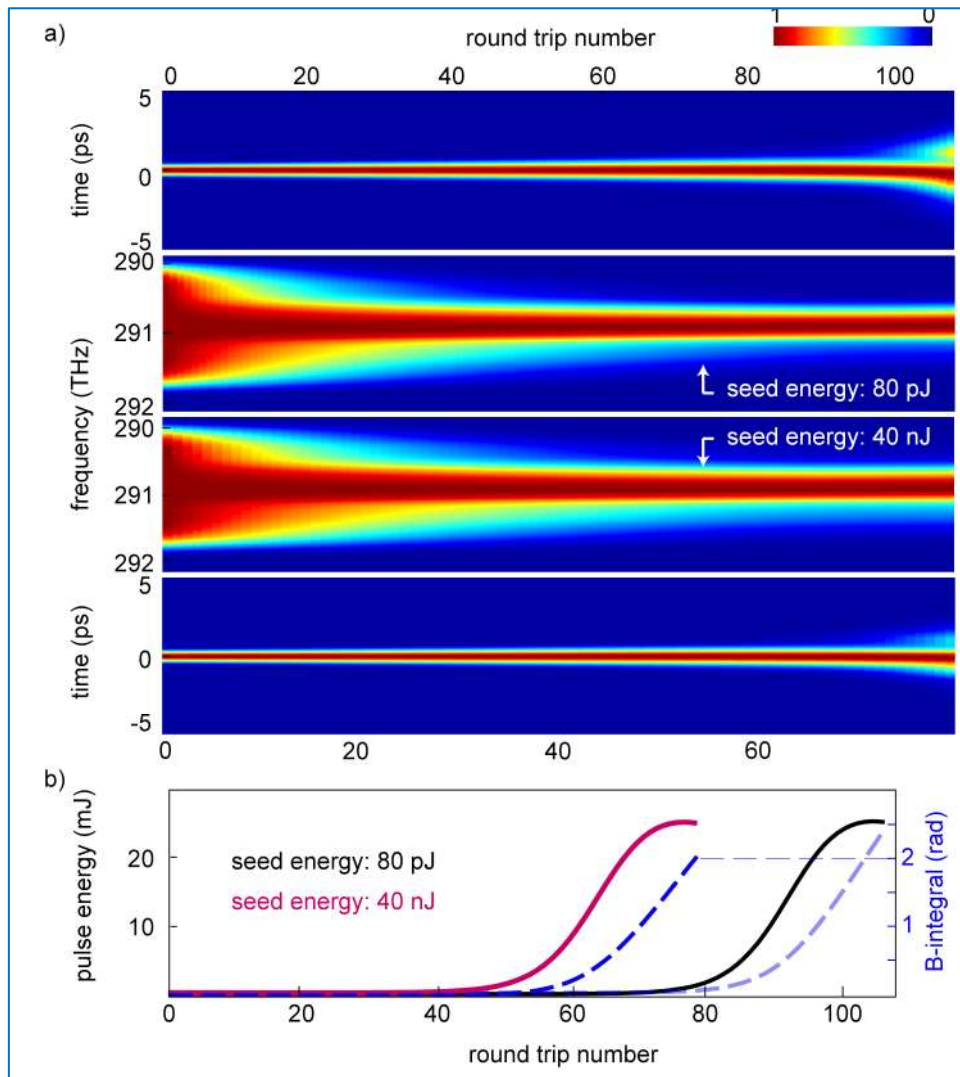

***Figure 2**. Influence of input seed level on final pulse quality in a thin-disk amplifier. Pulse-to-pulse coupling of amplification, Fig. 1, requires that the laser be operated well into saturation to avoid period doubling or chaos, but this increases the chance of accumulated nonlinear phase (B integral) harming the resulting pulse quality and stability of the peak laser power. (a) Amplification of 80 pJ seed pulses compared to 40 nJ seed pulses; the latter results in a slightly broader spectrum (less gain narrowing) and better temporal confinement of the pulse energy. (b) Comparison of the amplification of the two pulses: even though the energy of the pulse saturates at a given level, the B-integral does not saturate. If the B-integral significantly influences the spectral phase of the pulse, this will result in fluctuations in pulse duration and peak power, even if the energy noise is low in the saturated system. Adapted from [3]*

In addition to the changes mentioned above, the grating compressor was replaced with high-efficiency gratings on significantly thicker substrates (2 cm instead of 6 mm), with

correspondingly better surface flatness, improving the output mode and temporal profile of the resulting beam.

As a result of the above improvements, there were significant gains in laser performance. The RMS noise of the laser was reduced to 0.5% over a full day of operation (single-shot resolved detection with no temporal averaging). This was from the new cavity (Fig. 3), which reduced the final B integral to 0.5. The pulse duration reduced to 1.1 ps (from 1.6 ps previously), with excellent confinement of the energy to the main pulse, as shown in Figure 4. These changes have translated directly to increases in the stability and efficiency of the OPCPA.
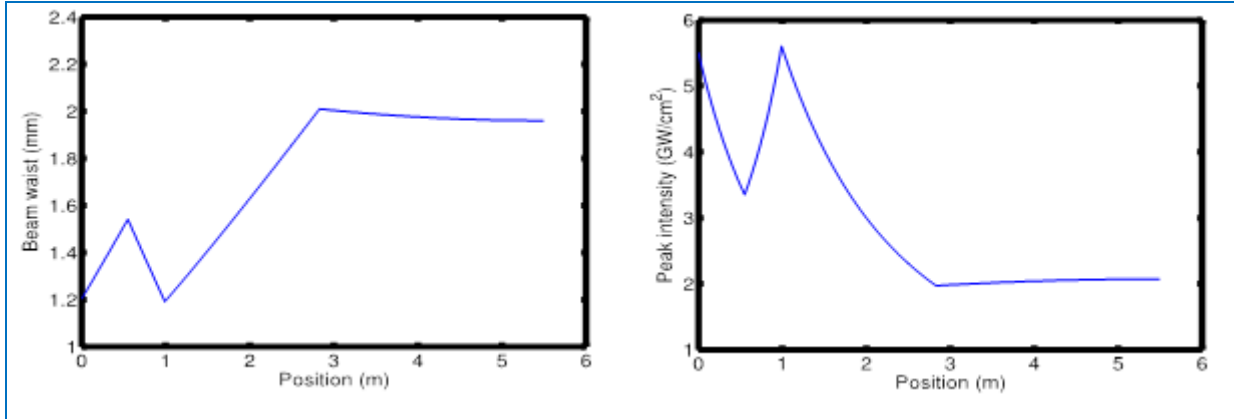

Figure 3. Improved cavity design of the regenerative amplifier, which was generated using a multivariable numerical optimization scheme designed to reduce the intensity on the cavity mirrors and Pockels cell, optimize the mode spot size on the gain medium, and minimize the alignment sensitivity and B integral.
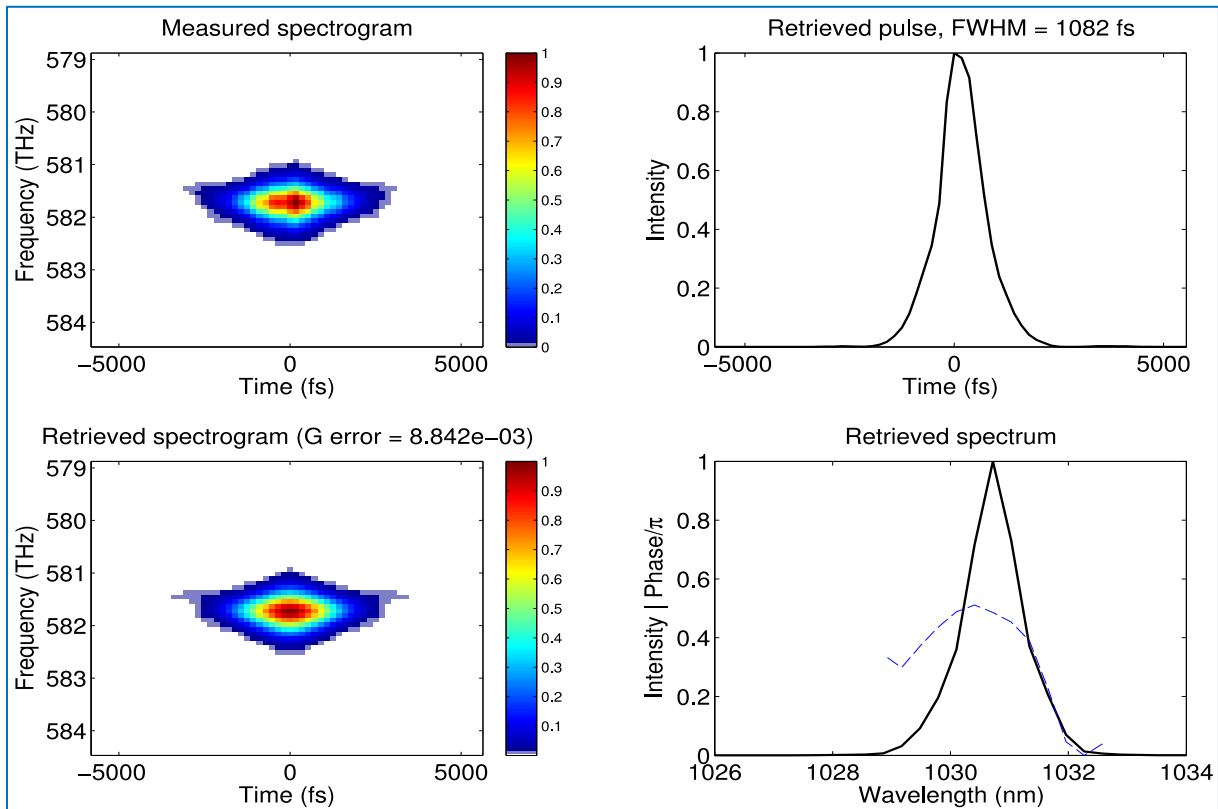

Figure 4. Second harmonic FROG trace of the pulse emitted by the Yb:YAG regenerative amplifier, with 1.1 ps duration.

✦ Conclusions

The attosecond infrastructure at MPQ based on OPCPA for the generation of high-energy infrared (2.1 µm) pulses and the associated diagnostics have improved to the point where the system is now being used for new experiments. Improved stability via the modified pump laser and access to the full temporal evolution of the electric field will enable exciting new experiments based on light-wave driven dynamics probed by high-energy attosecond pulses. These projects benefitted considerably both from the direct support of EUROLITE and the communication with expert researchers working on similar problems that it enabled.

✦ References

[1]   Y. Deng, A. Schwarz, H. Fattahi, M. Ueffing, X. Gu, M. Ossiander, T. Metzger, V. Pervak, H. Ishizuki, T. Taira, T. Kobayashi, G. Marcus, F. Krausz, R. Kienberger and N. Karpowicz, "Carrier-envelope-phase-stable 1.2 mJ, 1.5 cycle laser pulses at 2.1 µm," Optics Letters 37, 4973 (2013). dx.doi.org/10.1364/OL.37.004973

[2]   T. Metzger *et al.,* "High-repetition-rate picosecond pump laser based on a Yb:YAG disk amplifier for optical parametric amplification," *Optics Letters* **34**, 2123 (2009).

[3]   H. Fattahi, A. Schwarz, X.T. Geng, S. Keiber, D.E. Kim, F. Krausz and N. Karpowicz, "Decoupling chaotic amplification and nonlinear phase in high-energy thin-disk amplifiers for stable OPCPA pumping," *Opt. Express* **22**, 31440 (2014). 10.1364/OE.22.031440

3.1.2 High average power 100 kHz Fiber Chirped Pulse Amplification laser (CELIA)

✦ Objective

CELIA had the task to investigate the potential of ultrafast high repetition rate lasers for the generation of femto/attosecond XUV pulses with high average flux and high repletion rate. During LASERLAB III, CELIA improved and further characterised the home made fiber CPA Yb 100 kHz laser system.

✦ 50 W, Fiber based femtosecond CPA laser system.

We developed a high power Yb based Fiber Chirped Pulse Amplification (FCPA) laser system that operates at very high repetition rate (100 kHz). It is seeded with a Kerr-Lens Mode-locked (KLM) titanium sapphire oscillator emitting 7 fs pulses at 77 MHz. With the 300 nm broadband spectrum centred at 800 nm, a signal centred at 1030 nm is used to seed the FCPA Yb laser operating around 1030 nm.

The first amplifier is a 40 µm core air-clad Yb-doped photonic crystal fiber (PCF) having an inner diameter of 200 µm pumped with a 25 W laser diode emitting at 976 nm. The pulses are then stretched to a duration of 3 ns in a double-pass transmission-grating-based Offner stretcher (density 1750 l/mm).

The pulse train passes through two other pre-amplification stages based on the same design and a pulse picker which reduces the repetition rate to 100 kHz. The final amplifier is based on a rod-type PCF (80 µm Yb-doped core diameter, 200 µm double clad diameter) pumped with a 200 W fibre laser diode at 976 nm.

The amplified pulses are finally recompressed through a two-reflective-dielectric-gratings-based compressor (density 1760 l/mm) with a total efficiency of 90%.

The laser system delivers 570 fs pulse centred at 1030 nm, with 50 W average power at 100 kHz, resulting in 500 µJ pulse energy. Figure 5 displays the autocorrelation trace and the spatial profile of the amplified pulses.
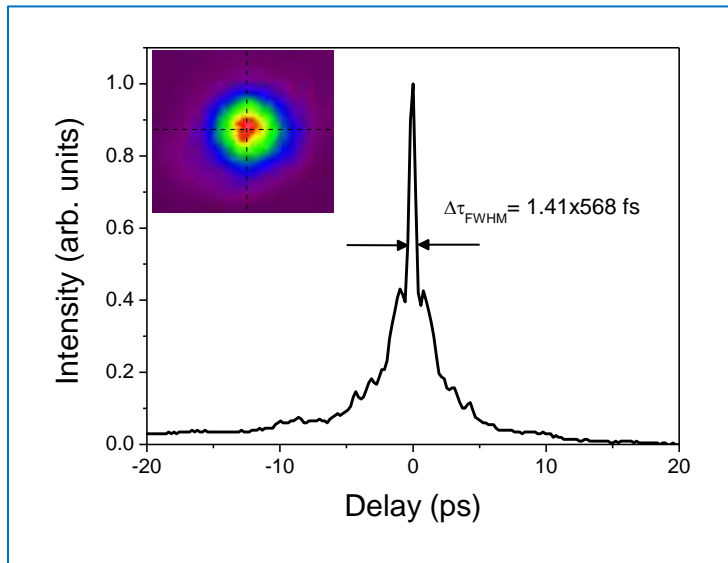

Figure 5. *Autocorrelation trace of the amplified pulses (inset: spatial profile of the laser beam similar to a Gaussian beam with M² = 1.3)*

Conclusions

Significant effort and progress have been made concerning the high repetition rate (100 kHz) FCPA laser system developed at CELIA. After characterization, its improved reliability allowed to observe and collect XUV light with up to 4×10^{10} photons per second at the output of the setup when harmonic were generated in Xenon (see section 3.2.1).

3.1.3 Post compression of TW laser pulses (CELIA)

Objective

A new scheme for post-compression of femtosecond laser pulses has been developed at CELIA specifically to go above the mJ level, the final goal being the generation of high energy attosecond pulses. This approach allowed to post compress TW pulses and to obtain, for the first time TW pulses with 10 fs duration.

Description of work

The original approach followed by the CELIA group is based on self-phase modulation induced by multiphoton ionization.

The experiment relied on a setup (Fig. 6) that was fully under vacuum (including the CPA compressor). The beam was guided in a 440 µm large diameter, 40 cm long capillary where Helium gas was injected at low pressure. Ionization of the Helium gas induced a time-dependent evolution of the gas index that led to a large spectral broadening. After the capillary, the beam diverged and was afterward collimated with a 6m focal length mirror. Recompression was achieved by using two pairs of chirped mirrors. A fraction of the pulse was then characterized with a single shot autocorrelator.
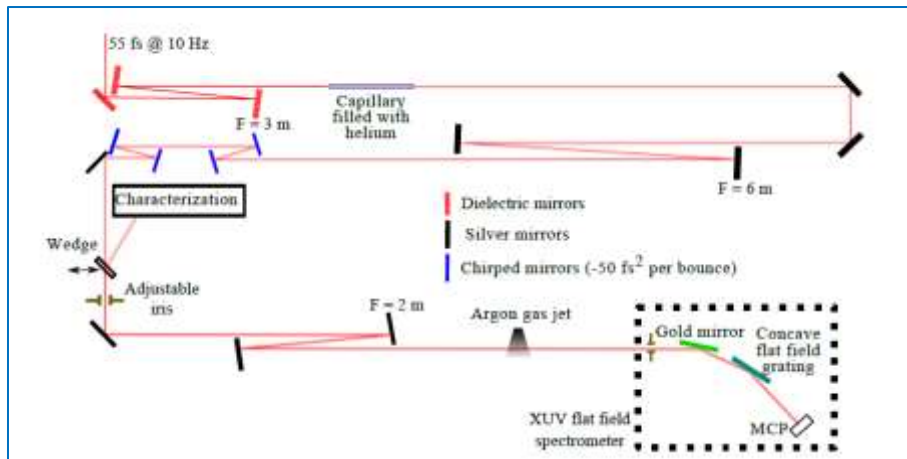
Figure 6. *Setup used for post compression of high energy TW pulses.*

The achieved pulse broadening did depend a lot on both the Helium pressure and pulse energy. After optimization, spectral broadening larger than ~4 could be obtained and spectra compatible with sub-10 fs pulses were recorded with high pulse energy (10 mJ or more).
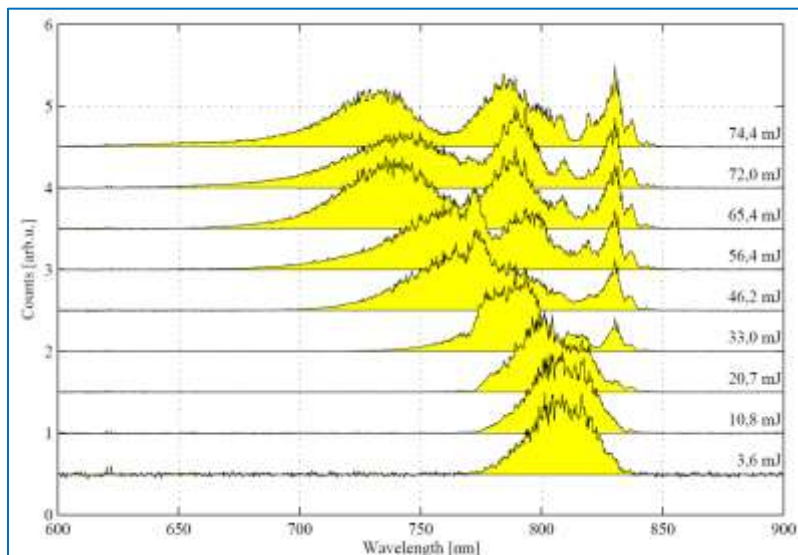

Figure 7. *Impact of the pulse energy on the spectral broadening of a pulse propagating in ionizing Helium (7 mbar).*

Recompression was achieved with two pairs of broadband chirped mirrors, that turned out to be very efficient in a large range of spectral broadening and allowed them to obtain 10 fs pulses (assuming a sech^2 pulse shape). As the number of reflections cannot easily be changed under vacuum, the tuning parameter was the Helium pressure.
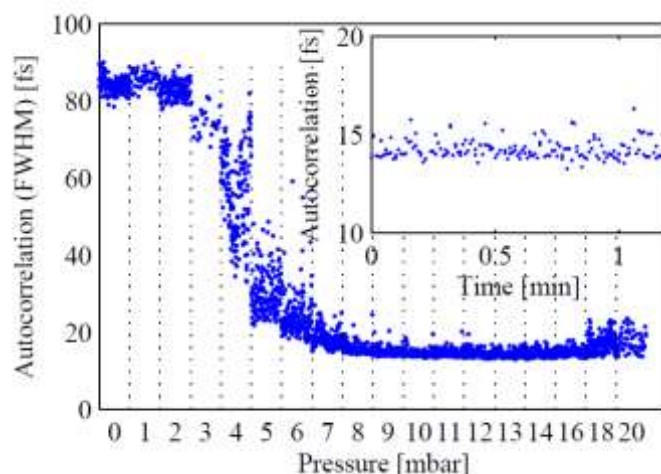

Figure 8. *Full width at half maximum (FWHM) of the single shot autocorrelation of the pulses as a function of the gas pressure.*

This experiment allowed CELIA to obtain 10 fs pulses with output energy of 10 mJ at a repetition rate of 10 Hz. It corresponds to 1 TW peak power and this energy level is above the capability of conventional post compression based on SPM via Kerr non linearity. This approach has even the possibility to be upscaled by using multiple ionisation and opens the post compression approach to TW lasers.

These pulses were used afterward to generate high order harmonics in gases and the high XUV signal obtained per shot confirmed that the high energy post compressed pulse have the proper characteristics to trigger coherent non-linear processes in large volumes of gases.

✦ Conclusions

Post compression of high-energy pulses was achieved by using ionization as a non-linear effect that induces SPM in a guided geometry. Ultrashort, 10 fs pulses were obtained at the TW level with high stability.

✦ References

[4]   Post-compression of high energy terawatt-level femtosecond pulses and application to high order harmonic generation", Ondrej Hort, Antoine Dubrouil, Amélie Cabasse, Stéphane Petit, Eric Mével, Dominique Descamps, and Eric Constant, JOSAB 32 (n°6), 1055 (2015) http://dx.doi.org/10.1364/JOSAB.32.001055

[5]   "Spatio–spectral structures in high-order harmonic beams generated with Terawatt 10-fs pulses", A. Dubrouil, O. Hort, F. Catoire, D. Descamps, S. Petit, E. Mével, V. Strelkov and E. Constant, Nature Communication 5:4637 (2014), http://dx.doi.org/10.1038/ncomms5637

3.1.4 OPA development and application to the generation of soft X-ray radiation in the water window (ICFO)

✦ Objective

The ICFO team is very active in the development of ultrafast and CEP controlled sources at high intensities and high average power. This operating regime is notoriously difficult to reach due to the absence of suitable gain media. The objective of the ICFO team was the development of one of the first few-cycle and CEP stable long wavelength drivers for attosecond generation in the water window regime.

✦ Mid-IR OPA associated with post-compression and/or cross polarized wave generation [5,6]

The ICFO team has, over the last years, developed a high average power Ti:Sapphire laser system capable of pumping a white-light seeded optical parametric amplifier which is followed by a gas-filled hollow fiber setup and compression at 1850 nm center wavelength. Current operating parameters are:

- Ti:Sapphire system: 35 fs pulse duration, 1 kHz repetition rate, 10 mJ energy
- OPA + broadening: 1.6-cycle pulse duration, 0.6 mJ energy, 1850 nm center wavelength, better than 80 mrad rms CEP stability during 72 h.

During LASERLAB 3, cross polarized wave generation at 2 µm was implemented to investigate how this method could push pulse durations towards the single-cycle regime and at appreciable pulse energy. The setup is displayed on Figure 9.
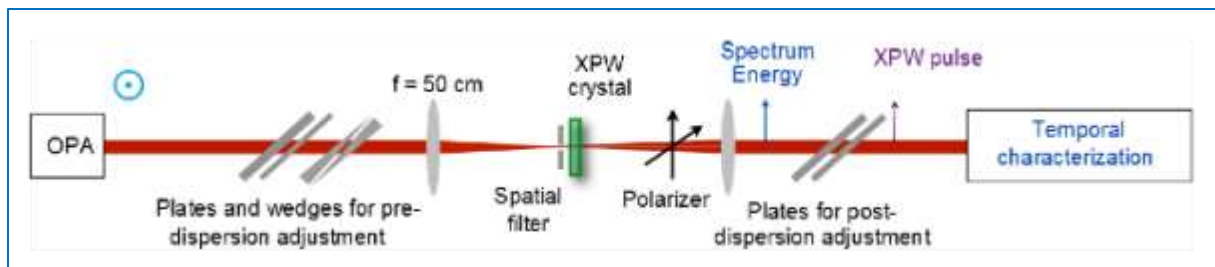
Figure 9. *set-up used for the XPW experiment.*

Figure 10 shows results from a first investigation which was conducted in collaboration with the team at LOA. Figure 11 shows part of the OPA setup, the hollow fiber broadening stage and the measured pulse duration at 1850 nm.
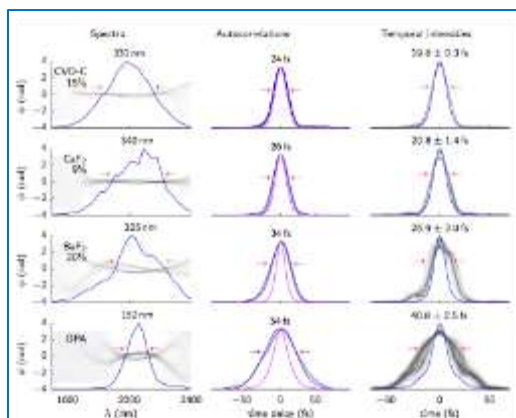

Figure 10. *Top, shown is the setup; Bottom, The performance of XPW was investigated for various host materials, this is important due to their varying dispersion characteristics and nonlinear coefficient. Achieved pulse durations varied between 6 and 2.8 cycles in this initial investigation.*

Figure 11. *Left, shown is the OPA setup; Middle, hollow fiber, pumped by 1 mJ 1850 nm; Right, FROG measurement of the sub-2-cycle pulse emerging from the hollow fiber compressor*

✚ Conclusion

As a further development of its mid-IR OPA, ICFO investigated XPW as a complementary technique to hollow fibre compression and achieved 6 to 2.8 cycle duration in an initial XPW study. The next step will consist in combining the hollow fibre setup with XPW to near the single-cycle high energy pulse regime.

✚ References

[6]   A. Ricci, F. Silva, A. Jullien, S. L. Cousin, D. R. Austin, N. Forget, J. Biegert, R. Lopez-Martens, "Generation of high-fidelity few-cycle pulses at 2μm via cross-polarized wave generation", Opt. Exp. 21, 9573, 2013.

[7]   H. Pires, M. Galimberti, G. Figueira, "Numerical evaluation of ultrabroadband parametric amplification in YCOB" Journal of the Optical Society of America B Vol. 31, Issue 11, pp. 2608-2614 (2014)
DOI: https://www.osapublishing.org/josab/abstract.cfm?uri=josab-31-11-2608

3.2   HHG produced XUV femto/attosecond pulses and attosecond beamlines

Optimising the High Harmonic Generation (HHG) process is central to efficient generation of attosecond pulses. CELIA developed a specific HHG set-up optimised for its 100 kHz laser driver while ICFO aimed at reaching the water window. MPQ constructed a complete and versatile attosecond beamline optimised for several types of applications such as attosecond streaking and transient absorption spectroscopy and high-field light-matter interaction.

While these partners used gas targets for the HHG, LOA and HIJ chose plasma targets. LOA developed an attosecond beamline based on few-cycle light-driven plasma mirrors at 1kHz and HIJ investigated the HHG on solid targets using a multi Terawatt (40TW) laser.

Finally, FORTH and HIJ investigated polarisation gating schemes to generate single attosecond pulses from multi-cycle laser drivers.

3.2.1   High repetition rate XUV generation (CELIA)

⁂   **Objective**

CELIA aimed at developing a HHG set-up optimised for its 50 W, 100 kHz FCPA laser driver.

⁂   **Description of work**

The output laser beam of the 50 W, 100 kHz FCPA laser driver described in section 3.1.2 was collimated to a beam size of W= 8 mm, transmitted through a half waveplate and polarizer to control the pulse energy and focused using a 200-mm focal length lens to perform HHG. The estimated beam size at focus is W_0 = 10.6 µm (with M^2 = 1.3) leading, at 50W, to an estimated maximum peak intensity of 5×10^{14} W/cm^2, high enough to perform HHG in gases.

The gas is supplied by two different kinds of geometries: a gas jet with an inner diameter of 200 µm or a semi-infinite gas cell of 40 mm length. The gas jet (or cell) is housed in a vacuum chamber pumped by a turbo pump. The emitted XUV beam is characterized by the XUV spectrometer which was capable to collect the harmonics and to withstand the 50 W average power of the FCPA laser without any damage (Fig. 12).
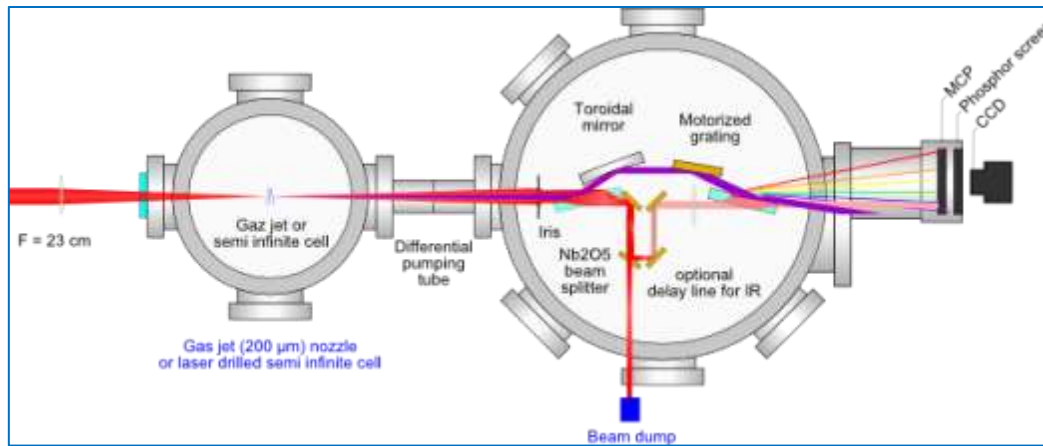
Figure 12. *Schematic view of the XUV generation chamber and the wide angle XUV spectrometer. After HHG, the IR and XUV are splitted and the XUV source is imaged onto a detector. The IR beam can be recombined with the XUV beam to perform pump probe experiments with spectral or temporal resolution with this IR/XUV interferometer.*

CELIA observed high order harmonics and recorded the XUV spectra emitted, in three different gases: argon, krypton and xenon. In a gas jet, the highest order harmonic, H29, was observed in argon and krypton. Harmonics from H11 to H23 were also produced and detected in Xenon. With a semi-infinite gas cell, odd harmonics have been produced in argon (up to H29), krypton (up to H29) and Xenon (up to H23).
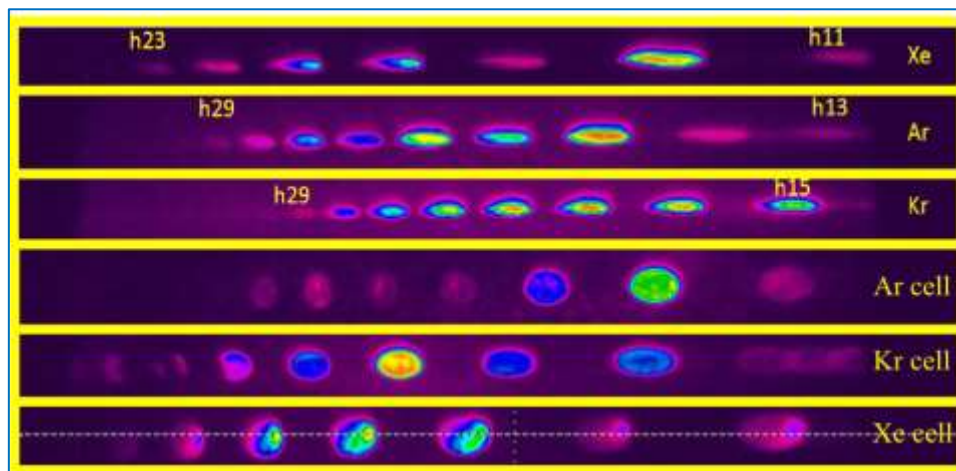

Figure 13: *Harmonic spectra observed after emission in a gas jet (top 3 figures) and a semi infinite gas cell (lower figures). The maximum order observed were 23 for HHG in Xenon and 29 for HHG in Ar or Kr and a spectral selectivity is observed for HHG in a gas cell.*

The maximum order observed was the same in both cases which indicates that the cutoff position was imposed by the single atom response and not by propagation.

In this case, the cutoff position can provide an estimate of the peak intensity where harmonics are produced. The cutoff law: $h\nu_{max} = I_p + 3.2\ U_p$ with $U_p = 10$ eV / 10^{14}W/cm^2 at 1030 nm (photon energy is 1.2 eV) gives a maximum intensity of 5×10^{13} W/cm^2 for HHG in Xenon and of $7\ 10^{13}$ W/cm^2 for HHG in Ar and Kr. These values are smaller than the estimated peak intensity and can indicate that either the peak intensity is overestimated or that HHG occurs before the peak of the pulse and is prevented when the atoms get ionized. This ionization occurs at low intensity with long pulses but if this was a limiting effect a

13

difference in the maximum cutoff order should then be observed between HHG in Ar or in Kr. It is also possible that the XUV spectrometer transmission decreases abruptly above 35 eV but the theoretical estimate disagrees with this possibility. The achieved peak intensity is therefore as high as 7×10^{13} W/cm^2.

The XUV signal was also characterised by using XUV diodes and thin Al filters. The number of detected XUV photons was high as we obtained 4×10^{10} photons per second at the output of the setup when harmonic were generated in Xenon (all harmonics above the 15th were refocused on the photodiode). We stress that this corresponds to the number of photons that can be used for experiments. As the transmission of our setup is of few %, the number of generated photons must be in the range of 10^{12} photons per harmonics per seconds and corresponds to an estimated flux of 1- 10 µW per harmonic. We also observed that the pulse duration is not detrimental for high power HHG and using 500 fs fundamental pulses is compatible with high XUV photon flux. This setup allowed us to observe that similar photon flux could be obtained with a jet or a semi-infinite gas cell in the tight focusing regime but the gas load is strongly reduced with a gas cell. We observed that the XUV beam characteristics are strongly dependent on the gas pressure and iris diameter. When a semi-infinite gas cell was used, controlling these parameters could lead to a clear spectral selection and to the generation of few predominant harmonics.

⬩ Conclusion

The laser development described in section 3.1.2 allowed CELIA to achieve high order harmonic generation with a 50 W, Yb fiber CPA source and collect XUV light with up to 4×10^{10} photons per second at the output of the setup when harmonic were generated in Xenon.

3.2.2 Generation of soft X-ray coherent radiation in the water window (ICFO)

⬩ Objective

ICFO sought to generate soft X-ray ultrashort pulses in the water window for applications in life science.

⬩ Description of work

The beamline described in section 3.1.4 was outfitted with a harmonic target which can be pumped with up to 6 bar of backing pressure in Helium. Using such a target, ICF achieved generation of coherent radiation beyond the oxygen k-shell edge (see Fig. 14). This is a significant step since one of the aims in attosecond science and strong field physics is to transpose attosecond pulses into the biologically relevant, so called, water window spectral range. This spectral range, between the carbon and oxygen k-shell edges (290 eV and 530 eV), is especially relevant for coherent diffractive imaging and x-ray absorption measurements on biological samples since absorption of water is minimized, thereby permitting high contrast measurements.
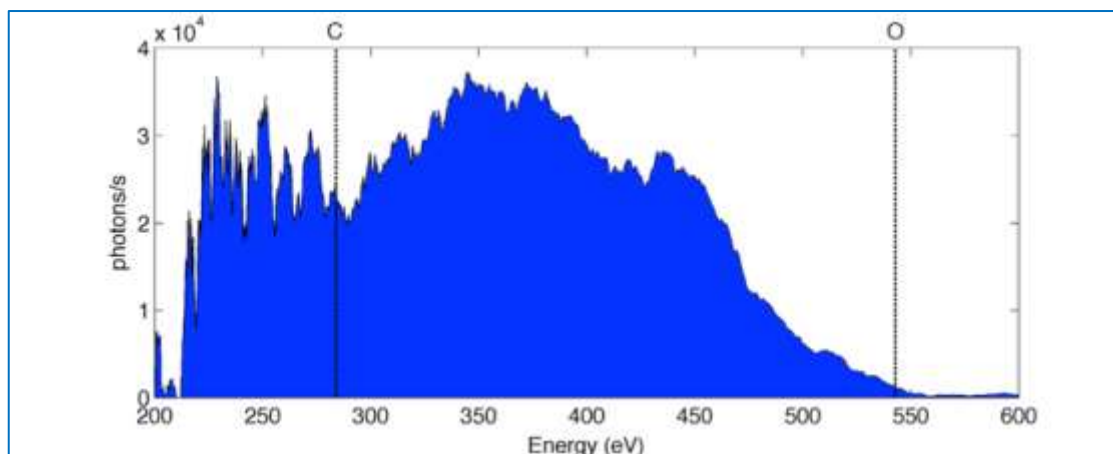
Figure 14. *Harmonic spectrum with calibrated photon yield from generation in 6 bar of helium. Indicated are the carbon and oxygen edges.*

Conclusion

ICFO developed a source, which is able to cover the entire water window spectral range up to the oxygen k-shell edge. Driving with a CEP stable sub-2-cycle source resulted in the first isolated attosecond soft X-ray pulse at 300 eV with a duration of 355 as [9].

References

[8]   S. M. Teichmann, F. Silva, S. L. Cousin, J. Biegert, "Importance of intensity-to-phase coupling for water-window high-order-harmonic generation with few-cycle pulses", Phys. Rev. A 91, 063817 (2015) DOI: http://journals.aps.org/pra/abstract/10.1103/PhysRevA.91.063817

[9]   F. Silva, S. M. Teichmann, S. L. Cousin, M. Hemmer, J. Biegert, "Spatiotemporal isolation of attosecond soft X-ray pulses in the water window", Nature Commun. 6, 6611 (2015) DOI: http://www.nature.com/ncomms/2015/150319/ncomms7611/full/ncomms7611.html

[10] S.L. Cousin, F. Silva, S. Teichmann, M. Hemmer, B. Buades, J. Biegert, "High flux table-top soft X-ray source driven by sub-2-cycle, CEP stable, 1.85 µm 1 kHz pulses for carbon K-edge spectroscopy", Opt. Lett. 39, 5383 (2014). DOI: https://www.osapublishing.org/ol/abstract.cfm?uri=ol-39-18-5383

[11] S.L. Cousin, F. Silva, S. Teichmann, M. Hemmer, J. Biegert, "Molecular fine structure from water-window coherent soft-X-rays", Opt. Photon. News 25, 58 (2014). DOI: http://www.osa-opn.org/home/articles/volume_25/december_2014/extras/molecular_fine_structure_from_water_window_x-rays/#.VinvQka2Vpu

3.2.3 TW, near-single-cycle pulses laser system and attosecond beamline from plasma mirrors (LOA)

Objective

The objective was to build an attosecond beamline based on plasma mirrors operating at 1 kHz.

Description of work

LOA has developed a kHz repetition rate beamline dedicated to the production of intense attosecond pulses from a few-cycle light-driven plasma mirrors. This beamline is now operational and has enabled the first pump-probe experiments on plasma mirrors to reveal

the anti-correlated emission of high-order harmonics and energetic electrons in the sub-relativistic regime [12]. The beamline also features a simple and general method, based on Spatial Domain Interferometry (SDI), for characterizing the plasma density ramp in-situ at the plasma mirror surface, which is essential for controlling the harmonic generation efficiency [13].

In the build-up towards this, LOA upgraded the "Salle Noire" TiS laser system into a double-stage CPA featuring a nonlinear filter to enhance the contrast of the pulses delivered on target. Today, the laser generates 10 mJ, 20 fs pulses with full CEP control and $> 10^{11}$ temporal contrast [14].

Moreover, an experimental LaserLab access campaign with Tamas Nagy (Laser Laboratorium Goettingen) was carried out to post-compress these pulses down to few-cycle duration using "long & stretched" hollow fiber technology. So far, this approach has produced 3.5 mJ, sub-4 fs pulses [15]. A new LaserLab campaign is currently underway using an all-vacuum setup in order to generate high-contrast TW peak-power waveform-controlled near-single-cycle pulses (> 3 mJ, ~ 3 fs).

Conclusion

LOA has developed a unique source that will be used to generate intense single attosecond pulses from plasma mirrors and perform nonlinear XUV spectroscopy applications for the first time at 1 kHz. In 2016, the beamline will be available for user-based LaserLab access campaigns.

References

[12]   On the correlated emission of high-harmonics and fast electron beams from relativistic plasma mirrors, M. Bocoum, B. Beaurepaire, A. Vernier, F. Boehle, A. Jullien, J. Faure, R. Lopez-Martens, manuscript in preparation.

[13]   Spatial-domain interferometer for measuring plasma mirror expansion, M. Bocoum, F. Boehle, A. Vernier, A. Jullien, J. Faure, R. Lopez-Martens, Optics Letters 13, 3009 (2015).

[14]   Carrier-envelope-phase stable, high-contrast, double chirped-pulse-amplification laser system, Jullien, A. Ricci, F. Böhle, J.P. Rousseau, S. Grabielle, N. Forget, H. Jacqmin, B. Mercier, and R. Lopez-Martens, Optics Letters 39, 3774 (2014)

[15]   Compression of CEP-stable multi-mJ laser pulses down to 4 fs in long hollow fibers, F. Böhle, M. Kretschmar, A. Jullien, M. Kovacs, M. Miranda, R. Romero, H. Crespo, U. Morgner, P. Simon, R. Lopez-Martens and T. Nagy, Laser Phys. Lett. 11, 095401 (2014)

3.2.4 HHG from multi TeraWatt lasers at 10 Hz (HIJ)

Objective

HIJ investigated the generation of coherent WUV pulses on surfaces using Ultra High Intensity lasers as driving lasers. The studies focused on laser contrast improvement, impact of the plasma density gradients and HHG characterisation with plane and structures surface targets. A broadband XUV polarimeter was also developed.

High repetition-rate plasma mirror for temporal contrast enhancement of terawatt femtosecond laser pulses by three orders of magnitude [16]

Achieving ultrahigh contrast is of prime importance for HHG on solid targets. HIJ investigated and characterised a plasma mirror that could operate at 10Hz.

The 40 TW laser JETI used at HIJ has an intensity contrast of 10^{-8} due to amplified spontaneous emission and prepulses with an intensity level of 10^{-5}. If the laser pulse is focused and intensities of 10^{19} W/cm² are reached a preplasma is created and the main pulse interacts with the plasma.

The principle of a plasma mirror is a femtosecond shutter that separates the amplified spontaneous emission and prepulses from the main pulse by focusing the laser pulse on a glass target. The intensity of the prepulses and the amplified spontaneous emission is not sufficient to create a plasma and is transmitted nearly completely due to an antireflection coating. The rising edge of the main pulse forms a plasma that reflects the laser pulse with enhanced contrast.
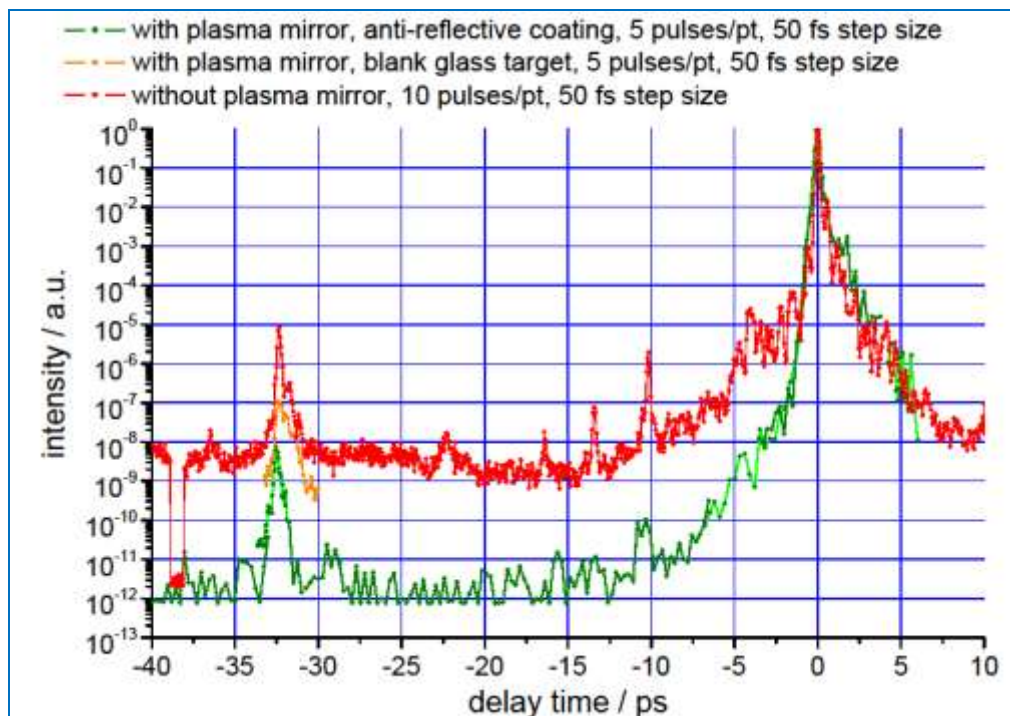

Figure 15. *Normalized intensity of JETI laser pulses measured with a THG autocorrelator*

A plasma mirror setup has been installed at the JETI laser system to enhance the pulse contrast in a controlled way. Two different plasma mirror targets are used: a blank glass target and a multilayer antireflection coated glass substrate. The multilayer antireflection coating has a residual reflectivity of 0.1 % which determines the contrast enhancement of 10^3. The pulse contrast for the different plasma mirror settings has been measured using a THG autocorrelator (s. Fig. 15).

Efficiency of high harmonic generation in the relativistic regime using ultra-steep plasma density gradients

HIJ investigated the efficiency of relativistic SHHG in experiments at the 40 TW laser system "JETI" using the plasma mirror. The harmonic radiation was measured using a calibrated XUV spectrometer [18].

As a first result, XUV pulse energies in the range of µJs and efficiencies of the order of ≈ 10^{-5} were obtained (s. Fig. 16). Thus, surface high-harmonic generation is becoming a competitive source to HHG in gases in terms of pulse energy and efficiency.

Second, a strong influence of the plasma scale length on the harmonics efficiency was found, which can be controlled by a tunable enhancement of the laser pulse contrast using the plasma mirror [17]. While rather steep plasma scale lengths are indeed a prerequisite for efficient surface high harmonic generation, our observations reveal – contrary to our expectations – that the efficiency of the harmonics declines for the steepest plasma gradients, i.e. the highest achievable laser pulse contrast [17]. Consequently, the harmonic efficiency can be optimized by a control of the preplasma conditions.
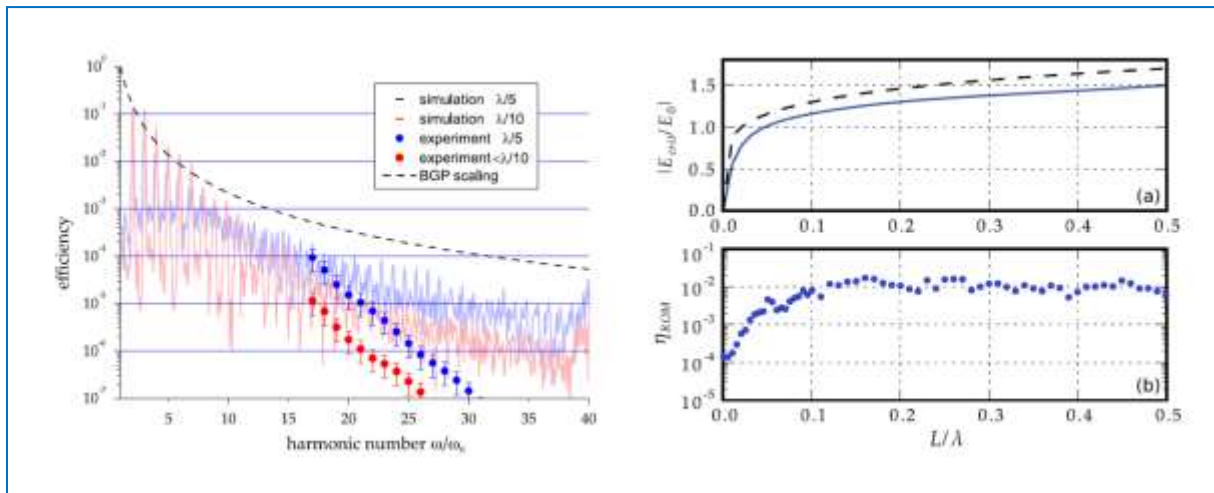

Figure 16. Left: Experimental efficiencies (circles) are compared to spectral densities from 1D laser-plasma simulations (lines) for different plasma scale lengths. Right: (a) The driving electric laser field at the plasmas surface as a function of the plasma scale length L. (b) Integrated harmonic efficiencies (above the 14th order) obtained from laser-plasma simulations.

The reduction of efficiency for ultra-steep gradients can be explained by two effects. Most prominently, larger restoring forces are present at the reflection point for extremely steep gradients thus suppressing the ROM process and efficiency. In addition, the electric field at the plasma-vacuum boundary is strongly attenuated for very plasma scale lengths (s. Fig. 16 right).

Generation of 10 µW relativistic surface high harmonic radiation with a repetition rate of 10 Hz

HIJ then measured for the first consecutively relativistic surface high-harmonic generation at a repetition rate of 10 Hz yielding an average power of 10 µW in the spectral range of 51 nm to 26 nm [18]. The laser pulses are frequency doubled using a nonlinear crystal (KDP). Through the nonlinear process of second harmonic generation, an excellent pulse contrast has been realized [19].
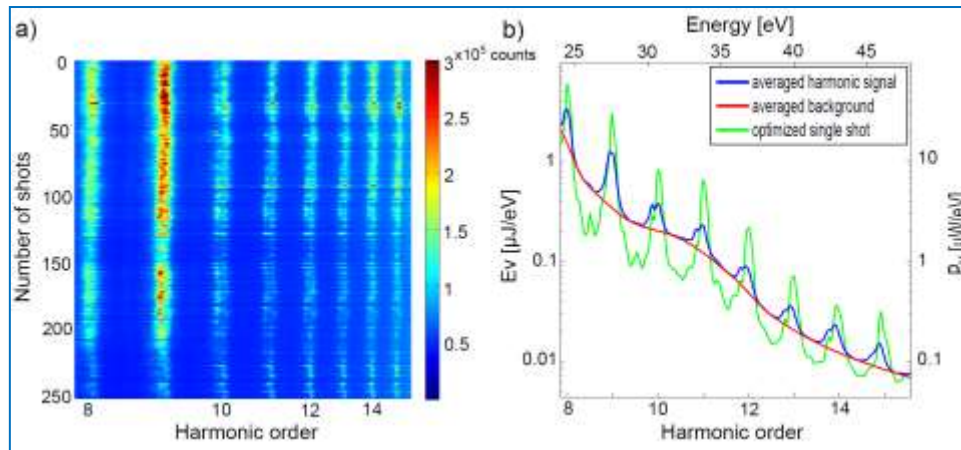
Figure 17. *a) XUV spectra generated by 250 subsequent laser shots at a repetition rate of 10 Hz. A false color scale is used for the number of counts. b) Averaged spectral energy per pulse and average power of the surface harmonics in comparison with the spectrum from a single shot under optimized conditions.*

Near-monochromatic high-harmonic radiation from laser plasma interactions with blazed grating surfaces [20]

Intense, femtosecond laser interactions with blazed grating targets were studied through experiment and laser plasma simulations. The high harmonic spectrum produced by the generation process is angularly dispersed by the grating leading to near-monochromatic spectra emitted at different angles - each dominated by a single harmonic and its integer multiples. The spectrum emitted in the direction of the third-harmonic diffraction order is measured to contain distinct peaks at the 9th and 12th harmonics which agree well with two-dimensional PIC simulations using the same grating geometry. This scheme appears to be a viable method of producing near-monochromatic, short-pulsed extreme-ultraviolet radiation.
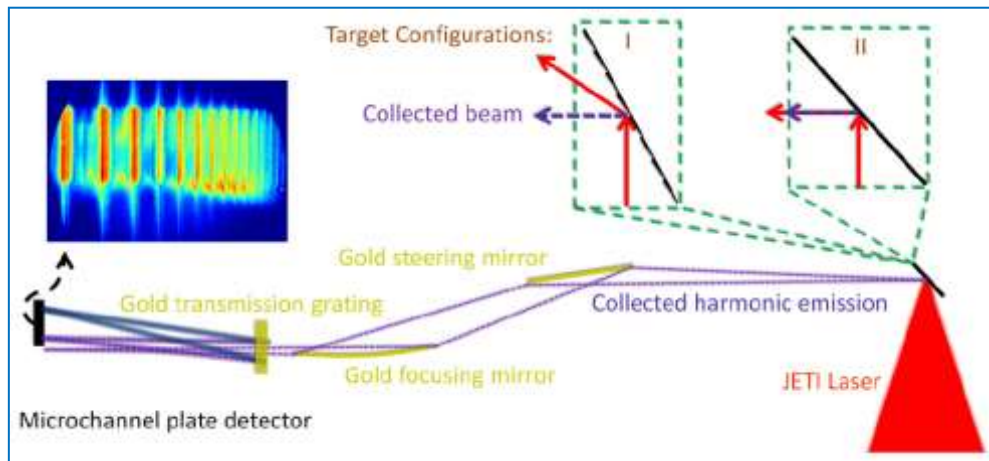

Figure 18. *Experimental setup: JETI laser pulses are focused on (I) a blazed grating target with the third harmonic's first diffraction order directed to the spectrometer or (II) a fused silica target reflecting the beam to the spectrometer in specular direction. The XUV radiation is collected by a steering and focusing mirror. The harmonic spectrum is recorded using a transmission grating and a CCD.*
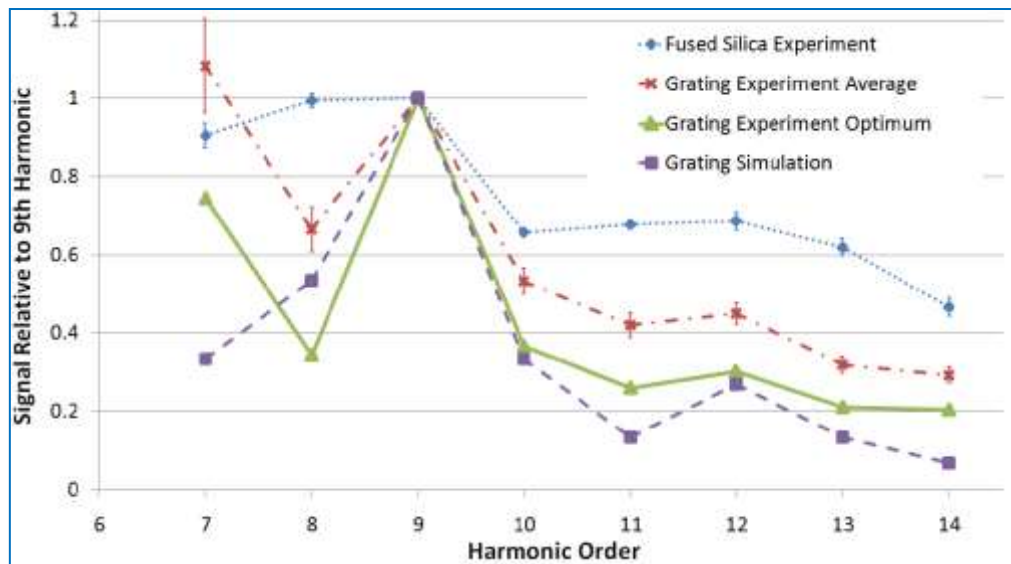
19

Figure 19. _Comparison of harmonic spectra obtained from the experiment and simulations: While the harmonic spectrum is decaying for higher orders for the fused silica target (case II), an enhancement of the 9th harmonic (slightly also the 12th) is found when the blazed grating configuration (case I) is used. The experimental results agree well with the harmonic spectrum obtained by a laser plasma simulation._

Broadband XUV polarimetry of high harmonics from plasma surfaces using multiple Fresnel reflections [21]

A broadband XUV polarimeter with an extinction rate of 5-25 for 17-45 nm has been developed. The Instrument was tested on a gas harmonic source and used to measure the polarization of high harmonics from plasma surfaces. The XUV polarimeter may also serve as a tool for polarization measurements of broad bandwidth XUV pulses—particularly for attosecond pulses from high-harmonic generation processes.
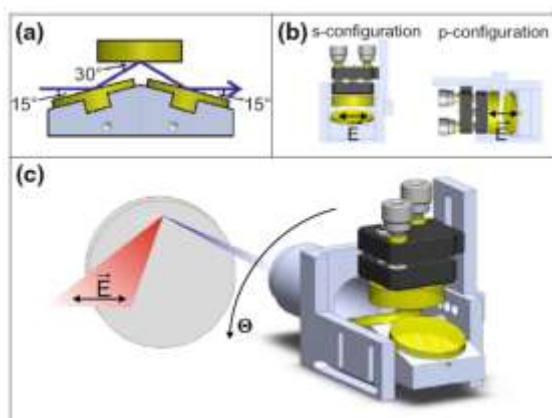

Figure 20. _a Grazing incidence reflections of the XUV beam at the goldcoated mirrors (15◦−30◦−15◦-configuration). b s- and p-configuration of the gold-coated mirrors relative to the expected electric field vector of the XUV beam. c Operational principle of the XUV polarimeter: The polarized broadband XUV beam is entering the polarimeter setup. Upon reflection at the three gold-coated mirrors, the XUV beam is attenuated. The transmission through the polarimeter setup strongly depends on the polarization relative to the incidence plane of the mirrors: transmission is significantly higher in s-polarization as compared with the p-polarized case_
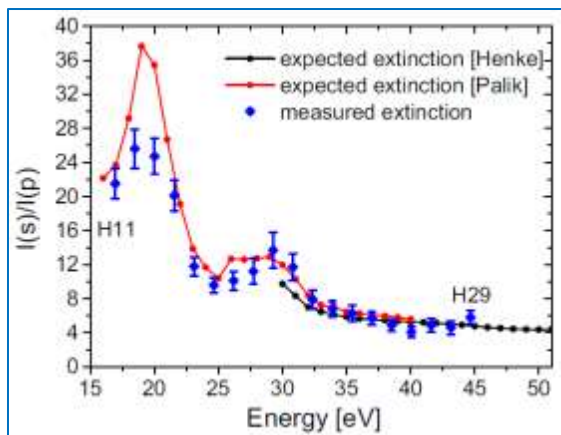
Figure 21. Measured extinction for H11 to H29 using surface high harmonics (blue dots). The measured values fit very well to the expected extinction when linearly polarized harmonics (p-polarized) are assumed (reflection calculated using data from Henke el al. [22] and Palik et al. [23]). The expected extinction ratio Is/Ip is approximately 5 for 35–50 eV (20–35 nm) and up to 25 for 20 eV (62 nm)

Conclusions

HIJ demonstrated that surface high harmonic radiation can be generated routinely with high efficiency when optimized laser and plasma parameters are utilised. The laser pulse contrast can be controlled by a single pass plasma mirror [16] or frequency doubled laser pulses [19]. High harmonic generation was realized with a repetition rate of 10 Hz. With the developed polarization diagnostic, HIJ could show that the polarization of CWE and ROM harmonics retain the p-polarization of the driving laser pulse. Moreover, the harmonic spectrum and direction can be controlled using blazed gratings as targets.

References

[16]   Rödel, C., et al., *High repetition rate plasma mirror for temporal contrast enhancement of terawatt femtosecond laser pulses by three orders of magnitude.* Applied Physics B-Lasers and Optics, 2011. **103**(2): p. 295-302.

[17]   Rödel, C., et al., *Harmonic generation from relativistic plasma surfaces in ultrasteep plasma density gradients.* Physical Review Letters, 2012. **109**(12): p. 125002.
DOI: 10.1103/PhysRevLett.109.125002 [no open access]

[18]   Fuchs, S., et al., *Sensitivity calibration of an imaging extreme ultraviolet spectrometer-detector system for determining the efficiency of broadband extreme ultraviolet sources* Review of Scientific Instruments, 2013. **84**(023101).

[19]   Bierbach, J., et al., *Generation of 10 mu W relativistic surface high-harmonic radiation at a repetition rate of 10 Hz.* New Journal of Physics, 2012. **14**.
DOI: 10.1088/1367-2630/14/6/065005 [open access]

[20]   Yeung, M., et al., *Near-monochromatic high-harmonic radiation from relativistic laser-plasma interactions with blazed grating surfaces.* New Journal of Physics, 2013. **15**(025042). DOI: 10.1088/1367-2630/15/2/025042 [open access]

[21]   Hahn, T., et al., *Broadband XUV polarimetry of high harmonics from plasma surfaces using multiple Fresnel reflections.* Applied Physics B, 2015. Volume 118, Issue 2 , pp 241-245. DOI: 10.1007/s00340-014-5977-9 [no open access]

[22]   B. L. Henke, E. M. Gullikson, J. C. Davis, Atomic Data and Nuclear Data Tables 54, 2:181–342 (1993). http://henke.lbl.gov/optical_constants/

[23]   E. D. Palik, *Handbook of Optical Constants of Solids*, (Elsevier Science & Tech, 1985). http://www.refractiveindex.info

3.2.5 Infrared Attosecond Beamline AS4 (MPQ)

✚   **Objective**

MPQ developed a versatile beamline optimised for applications in ultrafast science such as attosecond streaking and transient absorption spectroscopy.

✚   **Description of work**

Making use of the laser system described in section 3.1.1 for attosecond science requires a dedicated beamline shown in Figure 22, which we have constructed at MPQ, primarily through household funding and funding from the Munich Centre for Advanced Photonics.
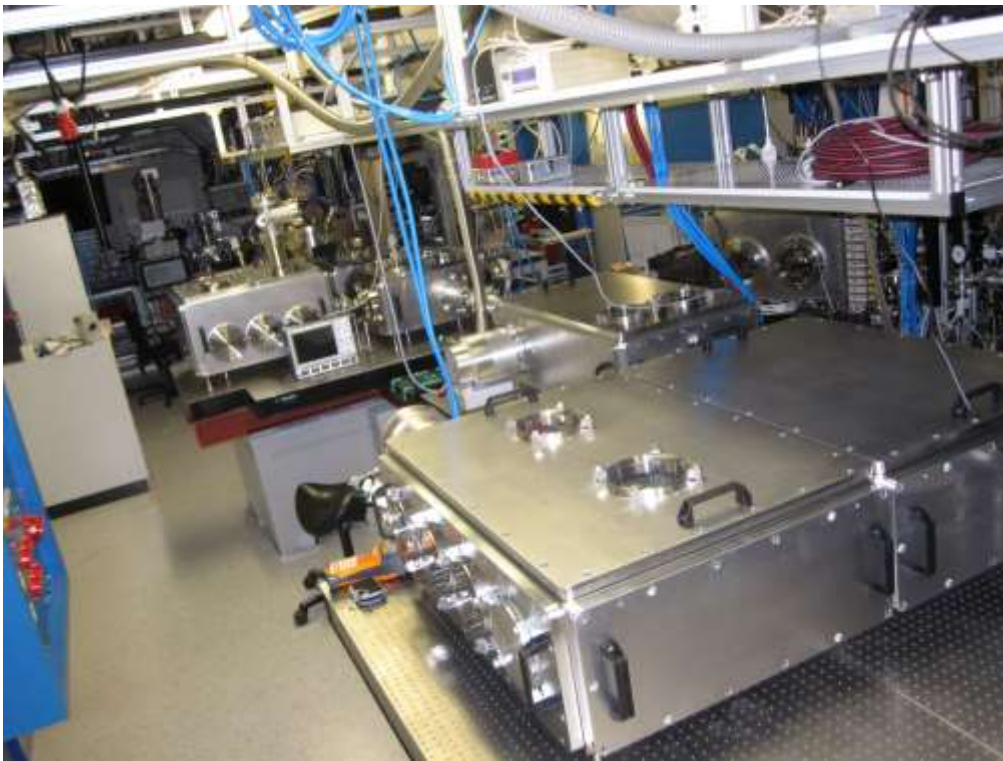

***Figure 22.** photograph of the AS4 beam-line at MPQ.*

The complex of five vacuum chambers is dedicated to five main tasks, in order: spectral broadening and waveform synthesis, high harmonic generation, temporal and spectral management of the attosecond pulses, attosecond streaking and transient absorption spectroscopy, and laser-field-controlled high-field light-matter interaction, shown in detail in Figure 23.
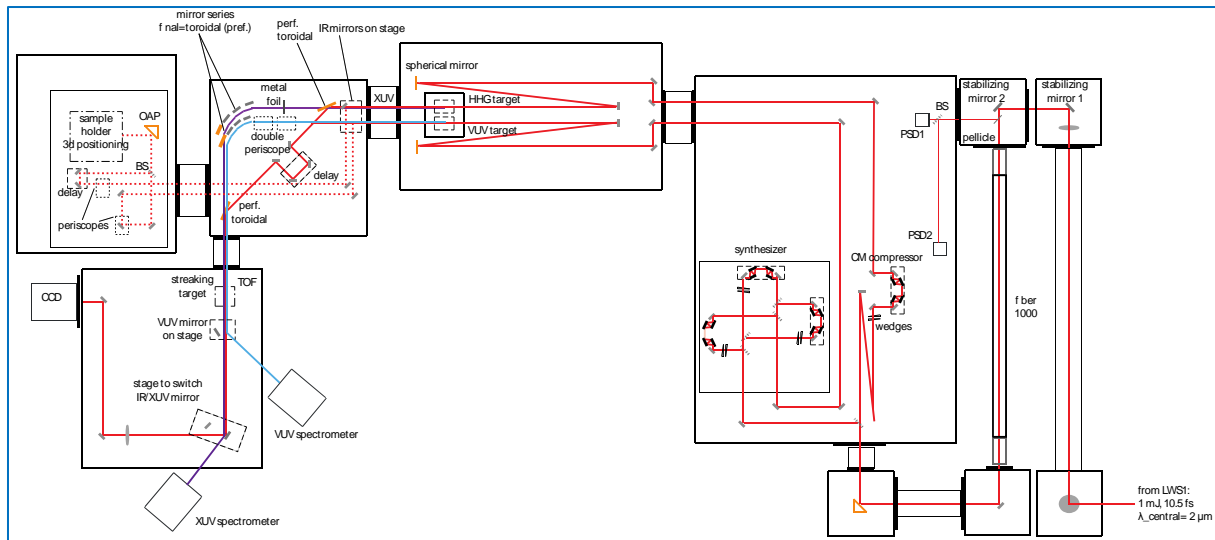
Figure 23. *Layout of the AS4 beam-line at MPQ.*

The five main chambers will be used for: 1) infrared light wave synthesis, 2) HHG 3) attosecond pump-probe delay, 4) attosecond streaking and spectroscopy, and 5) solid state attosecond physics. The system was designed to allow for very flexible implementation of new diagnostics and beam modifications in the synthesis chamber, combined with a compact beam transport after the high-harmonic target for improved stability compared to neighbouring beamlines.
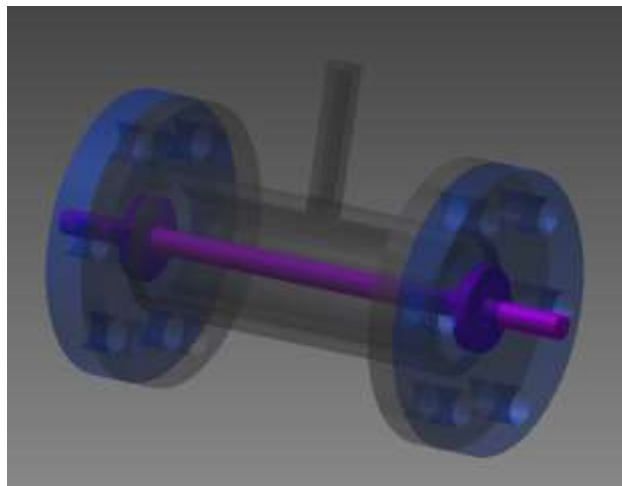

Figure 24. *New high harmonic target based on hollow core fiber. The fiber contains multiple laser-drilled inlets in the center portion, allowing for nearly-constant gas pressure in the central interaction length, and sits in a v-grooved steed rod (in violet) and sealed at the ends. This protects the outer chamber from vacuum load (the only gas exit is through the fiber itself), and the system is capable of holding tens of bar of backing pressure.*

The beamline is currently still in the development stage, as work is being performed to explore the generation of attosecond pulses with this unique light source. A new high harmonic generation target, shown in Figure 24, uses a short hollow-core fibre with multiple gas inlets to provide guided interaction between the laser pulse and gas, while simultaneously allowing for higher backing pressures to be used without overloading the vacuum pumps of the surrounding chamber. This results in efficient harmonic generation at

reduced backing pressures, as illustrated in Figure 25, with nearly-negligible gas load placed on the surrounding chamber.
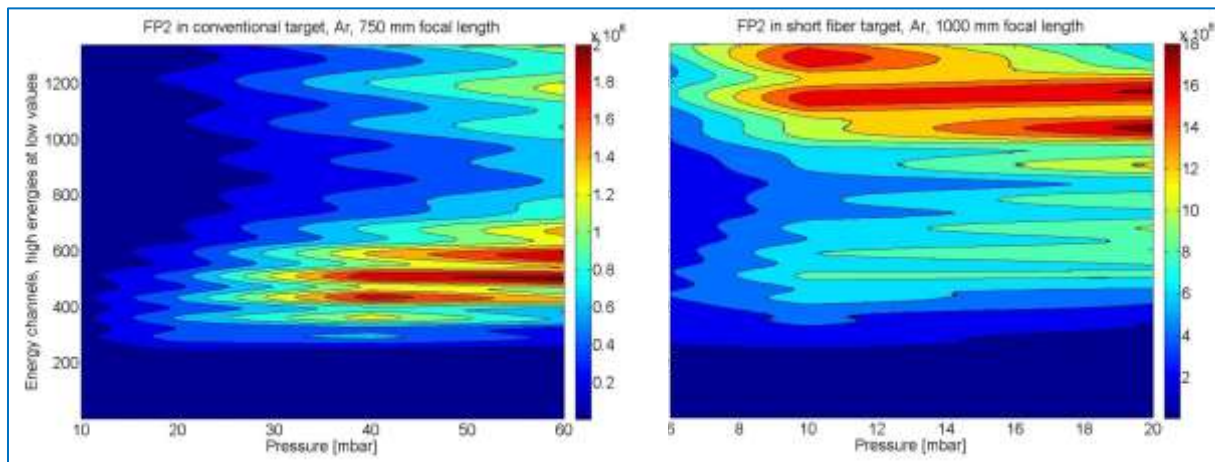

Figure 25. Difference in HHG characteristics in the fiber target (right) compared to conventional steel tube target (left). The fiber target's emission is optimized at lower backing pressures, but provides comparable flux.

✦ Conclusion

Intensive development has been carried out at MPQ to develop a specific attosecond beamline with optimised HHG and stability. This system will allow experiments that take full advantage of the specification of the MPQ OPCPA driving laser.

3.2.6 Polarisation Gating for the generation of isolated attosecond pulses from multi-cycle driving lasers (HIJ and FORTH)

✦ Objective

The objective is to demonstrate and use the possibility to generate energetic XUV super-continua confined in isolated pulses with sub-fs duration from multi-cycle driving lasers through the polarisation gating technics. As energetic XUV pulses are here defined pulses that can induce two-XUV-photon processes.

✦ Noncollinear polarization gating of attosecond pulse trains in the relativistic regime at HIJ [24]

HIJ implemented a method to temporally gate attosecond pulse trains by combining noncollinear and polarization gating. This scheme allows the pulse gating technique to be applied at the high beam fluence of multi-TW to PW class laser systems to generate isolated attosecond pulses. Unfortunately, with the 30fs pulses of the Jeti laser system the generation of isolated attosecond pulses could not be shown. But a significant spectral broadening was observed, which is in good agreement with predictions and demonstrates the effectiveness of this gating scheme. These results suggest that with pulses from existing high power laser systems such as the LWS20 and future systems such as the sub-20fs JETI200 system at the Helmholtz-Institute in Jena it will be possible to create isolated attosecond pulses.
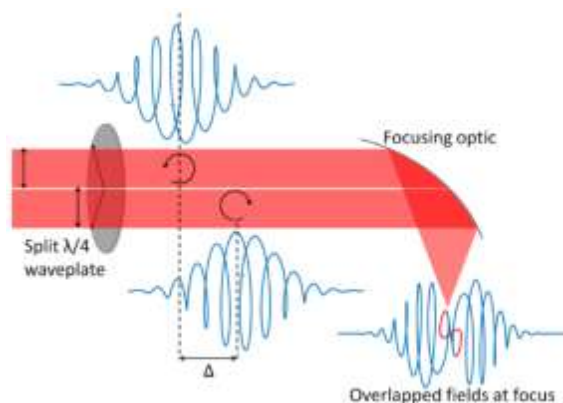
Figure 26. *Sketch of the noncollinear polarization gating method. A split quarter waveplate with orthogonal optical axes converts two delayed linearly polarized half beam pulses into left and right circularly polarized pulses. These pulses overlap at focus and create a linear gate.*
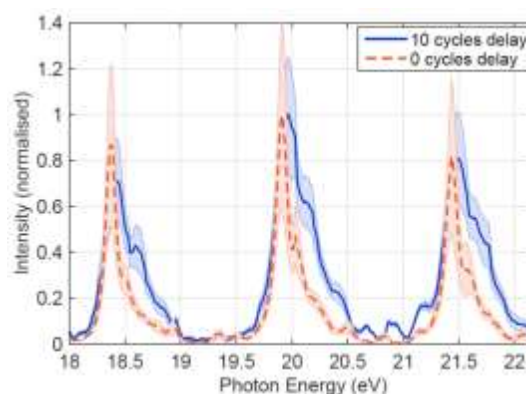

Figure 27. *Experimental high harmonic spectra averaged over 10 shots whilst using the split beam gating setup. The spectrum for harmonics 12 to 14 are shown for delays of 0 (dotted) and 10 (solid) cycles between the split beams and have been normalized to the zero delay peak of the 13th harmonic. The shaded region indicates the RMS signal variation.*

Generation of energetic XUV pulses with sub fs duration and application [25-27] (FORTH)

The generation of energetic attosecond pulses is highly desirable as it allows the use of proper characterization approaches of such pulses, as well as the implementation of XUV-pump-XUV-probe experiments, thus allowing the study of intrinsic dynamics of a system, avoiding distortion of it by the IR radiation used so far in two colour (XUV, IR) pump-probe schemes. The generation of XUV super-continua by few cycle pulses CEP stabilized pulses, allowing the observation of non-linear processes in the XUV, is not yet achieved. However, many cycle high peak power lasers supported by appropriate technologies allow the generation of such pulses. This is based on long focal length generating geometries and utilization of the so called Interferometric Polarization Gating technique developed at FORTH.

During the last reporting periods, FORTH has demonstrated the generation of energetic XUV super-continua confined in sub-fs pulses. The high energy of the pulses was verified through the first XUV-pump-XUV-probe studies of 1fs scale atomic and molecular dynamics.

For an improve performance of the attosecond beam-lines at FORTH an upgrade of the driving laser system has been finalized. The laser system has been installed in a new laboratory space. The oscillator is a CEP stabilized one. Two brunches are operational. The one brunch delivering pulse energies of 400mJ and pulse durations of 18fs at 10Hz repetition rate and a pulse contrast 10^{-9} at ns and 10^{-5} at ps. The second brunch is delivering pulse energies of 3mJ at 1kHz repetition rate and 18fs pulse duration. None of the amplified branches is operating yet under CEP stabilized conditions. An attosecond beam-line with 3m focusing elements is assembled and operational. A second new beam-line allowing for longer focusing conditions (up to 12m) is still under construction. Its main chambers are constructed. The beam-line will allow the use of the full laser energy available. Its assembling has started. The lab is operational and the first experiments related to the deliverable are targeting the generation of circularly polarized higher harmonics from laser aligned

molecules. For the 7th harmonic produced in aligned CO_2 molecules the process has been already demonstrated.

During the move of the lab and the installation of the upgraded laser system and of the beam-lines auxiliary work has been performed. Namely:

- A new compact collinear polarization gating set-up appropriate for many cycle pulses has been developed.
- Modelling work towards single shot non-linear auto-correlation has been performed and effects of long and short trajectories in the HOHG process have been studied. Currently the generation of circularly polarized HOH is studied in the new lab.

✛ Conclusions

HIJ work on noncollinear polarization gating showed promising results for isolated attosecond pulse generation at multi-TW to PW class laser systems with pulse durations shorter than 20fs.

Continuing the work on the generation of energetic XUV super-continua allowing two-XUV-photon processes and providing attosecond temporal resolution, upgrades of the laser system and the attosecond beam-lines have been implemented at FORTH and modelling work for related devices has been performed.

✛ References/Publications

(Publications resulting from the JRA need to indicate DOI and whether open access will be/is granted (yes/no). Please, remember the Laserlab acknowledgement.)

[24] Yeung, M., et al., Noncollinear polarization gating of attosecond pulse trains in the relativistic regime, Physical Review Letters, accepted on 15th Oct

[25] "Single-shot autocorrelator for extreme-ultraviolet radiation" G. Kolliopoulos, P.Tzallas, B. Bergues, P. A. Carpeggiani, P. Heissler, H. Schröder, L. Veisz, D. Charalambidis and G. Tsakiris. J. Opt. Soc. Am. B 31 (2014)

[26] "Unravelling the quantum optical underpinnings of high-order harmonic generation" K. Kominis, G. Kolliopoulos, D. Charalambidis and P. Tzallas , Phys. Rev. A89, 063827 (2014)

[27] "Revealing quantum path details in high-field physics" G. Kolliopoulos , B. Bergues, H. Schröder, P. A. Carpeggiani, L. Veisz, G. D. Tsakiris, D. Charalambidis and P. Tzallas Phys. Rev. A90, 013822 (2014)

3.3 CEP stabilisation and measurement

Controlling the Carrier-Envelope Phase (CEP) of the driving laser is a prerequisite to stable generation of attosecond pulses through High order Harmonic Generation. Within the Eurolite project SLIC pursued studies on CEP stabilization using the Electro Optic effect to control the CEP; the developments focused on the implementation of a fully analogical loop to increase the correction bandwidth and on the test of a new configuration to ensure isochronous CEP stabilisation. MPQ extended the electro-optic sampling (EOS) technique to the near infrared, allowing for direct access to near infrared electric field waveforms. Finally, HIJ demonstrated the possibility to performed a single-shot CEP measurement of a 40 TW laser at 1Hz using an ATI phasemeter.

3.3.1 Large bandwidth loop for improved CEP stabilisation demonstrated at SLIC

Objective

SLIC continued to investigate the potential of Electr-Optic phase-shifters in two directions. The first work aimed at implementing a fast CEP diagnostic in the CEP control loop in order to extend the correction bandwidth and achieve improved CEP noise reduction. This work has been carried out in collaboration with the CUSBO (Milano) and the Amplitude-Technologies company. The second part of the work consisted in modelling and implementing a new configuration ahieving isochronous phase shifting.

Large bandwidth loop for improved CEP stabilisation

The stabilization loop was developed at SLIC with Amplitude-Technologies and in collaboration with CUSBO. In order to get a loop operating at faster rate, we chose to build a fully analogical loop based on a specific f-2f set-up that is shown in figure 28 and is comparable to the system proposed and implemented by the Steimeyer group at MBI [28]. The key point of this system is that the CEP drift is measured through an error signal generated by 2 Photo-Multipliers Tubes (PMTs). It can thus be acquired at very high repetition rate since no digital data processing is required.
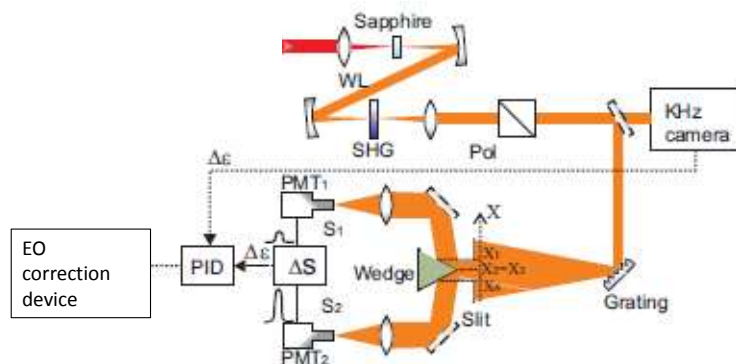

Figure 28. Experimental setup. SHG : second harmonic generation crystal; Pol: polarizer; PMT: photomultiplier; PID: proportional-integrative-derivative

After extensive tests in SLIC, this set-up was used to stabilize the CEP of a 20W, 10 kHz, 25fs TiS laser available in CUSBO (Milano) in the group of G. Sansone. The whole experiment set-up is provided in figure 29. The CEP stabilization can be done using either an Acousto-Optic Programmable Digital Filter (Dazzler from FASTLITE™) or an EO crystal (LiNbO$_3$). For the CEP measurement, we used either the CCD camera (with numeric data processing) or the analog detection device. This allowed for crossed comparison between our loop (EO crystal + analog loop) and a numeric one (CCD camera + Dazzler).
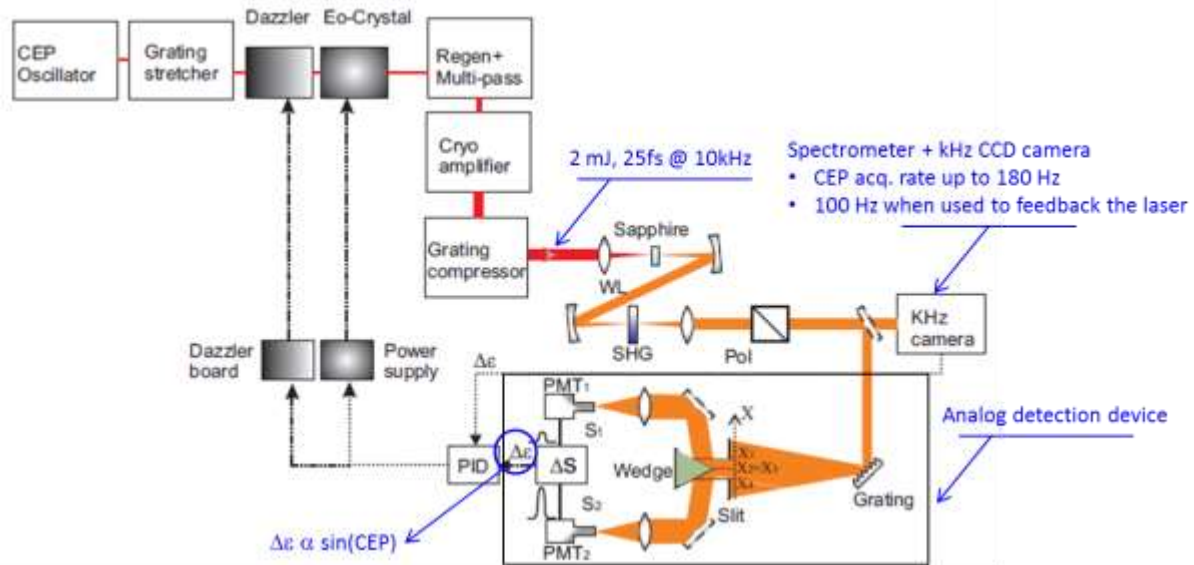
Figure 29. *experimental set-up for CEP stabilization of the TiS laser in CUSBO.*

The single-shot measured CEP drift using the feedback loops based on the PMTs and kHz camera acquisition systems are shown in Figure 30 [29]. In both cases, the CEP noise introduced by the amplification is controlled using the EO crystal. When using the kHz camera to feed the CEP stabilization loop, the sampling rate is reduced to 100 Hz, due to the software processing time. The measured CEP single shot standard deviations are 560 mrad when using the CCD camera and drop to 320 mrad when the PMTs based feedback loop is applied. These values are based on single-shot measurements to ensure meaningful comparison between data acquired with different detection systems and actuators.
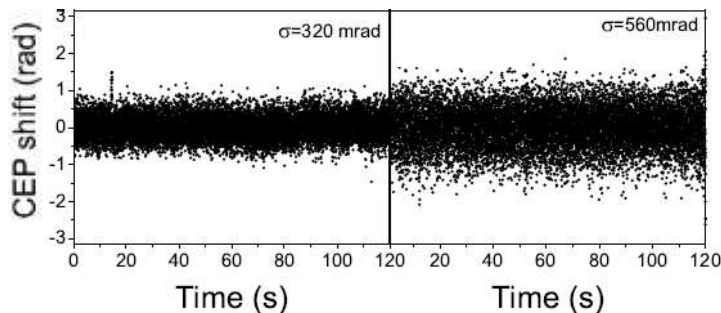

Figure 30. *Single-shot CEP variation measured by the kHz camera. The feedback signal correcting the noise introduced by the amplifier system was provided by the PMTs (left) or the kHz camera (right) detection systems acting on the EO crystal.*

The improvement in terms of bandwidth of correction can be seen on figure 28 which compares the power spectral densities (PSDs) of the CEP noise when using the CCD camera or the analogic set-up with the PMTs [29]. The PSDs without feedback on the amplifier are also shown for comparison (red curves). The kHz camera feedback loop allows to efficiently reduce the CEP noise up to about 10 Hz (Fig 31a); higher frequency components are not affected by the feedback loop due to the limited sampling rate of the error signal. The PMTs feedback, on the other hand, shows a reduction of the CEP noise up to the limit of 90 Hz (Fig 31b), imposed by the sampling rate of 180 Hz of the measurement. Figure 31c displays the PSD of the PMTs' difference signal error signal $\Delta\varepsilon$ (proportional to the sine of the CEP drift). One can see that the correction bandwidth extends beyond 100Hz. The phase noise integrated over the frequency range (blue-dashed curves) confirms that the

PMTs based feedback allows for a better control of the CEP with respect to the kHz camera system.
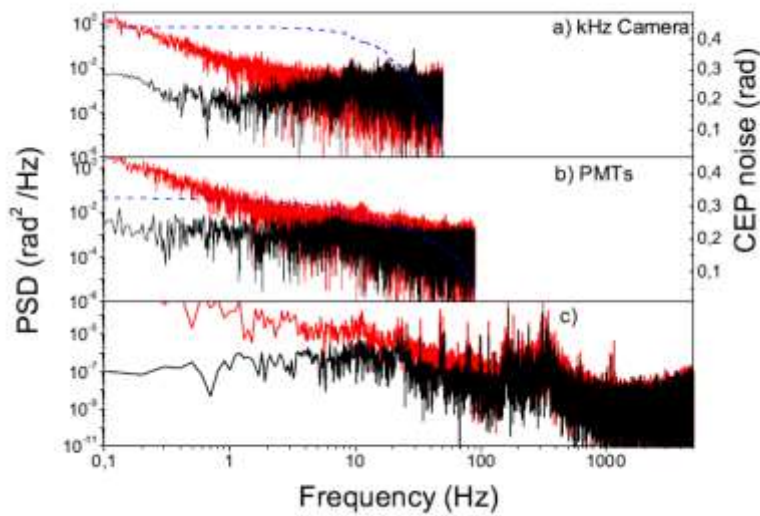

Figure 31. Power spectral density measured by the CCD camera with (black) and without (red) feedback loop operating on the amplifier. The error signal was provided to the CEP control device by the kHz camera (a) or by the PMTs (b). Power spectral density measured by an oscilloscope sampling the error signal with (black) or without (red) feedback on the amplifier (c).

Isochronous CEP shifter

A few years ago, SLIC proposed an original method based on the linear electro-optic (EO) effect in a bulk material ($LiNbO_3$ - lithium niobate, RTP - rubidium titanyl phosphate). In such a crystal, the refractive index can be linearly modulated by an external electric field, leading to a variation of the CEP. After demonstrating the principle of this method [30], this was successfully applied to the CEP control of a titanium-sapphire CPA laser [31]. Compared to the main equivalent systems, EO CEP shifters do not need mechanical displacements and have potentially a high correction bandwidth.

The previously described "bulk" EO CEP shifter is however neither rigorously isochronous (for an isochronous system, the electric field-induced group delay $\Delta\tau_g = 0$), nor iso-dispersive (for an iso-dispersive system, the electric field-induced dispersion $\Delta\Phi_2 = 0$). SLIC thus introduced a new set-up [32], still based on the EO effect, but which relies on the use of an EO dispersive prism pair. The idea was to combine material with angular dispersion, as in the case of a prism compressor. The prisms are EO crystals (RTP or LiNbO3 for example) on which an electric field is applied. Modeling of this new set-up was described in [32] where the analytical derivation of the spectral phase, of the group delay and of the CEP variation, as a function of the EO coefficient r_{33} (unclamped EO coefficient at λ_0) was detailed.

The experimental validation of the concept was done more recently with RTP prisms and results compared to former analytical predictions. To qualify the RTP prism pair EO set-up (prisms provided by Cristal Laser, France), and measure the CEP shift and the induced group delay, we used spectral interferometry [33] with a 84 nm (FWHM) spectral bandwidth, 800 nm Ti:sapphire laser source. The principle is to combine (here in a Michelson interferometer) a test and a reference beam with a given delay and send them into a spectrometer. The observed resulting fringed spectrum contains information related to the spectral phase difference between the two beams.

The geometrical arrangement is given on Fig. 32a. On Fig. 32b, one defines the prisms and the geometrical parameters d_2 (distance covered by the ray between the two prisms in air)

and d_3 (total path inside the prisms for the ray at the carrier angular frequency ω). Because the mathematical modeling leads to simpler analytical results and the optical alignment is easier, the particular case of minimum deviation for λ_0 was chosen. Two specific geometries were considered:

- CEP shift generation without variation of the group delay (Isochronous configuration)

- Group delay generation without variation of the CEP ("Pure Group Delay" - PGD - generation.

Each one corresponds to a specific condition to be satisfied by d_2/d_3. An excellent agreement was observed between the model and the experiments. In the PGD configuration ($d_2 = 40$ mm), when applying an electric field of ± 1000 V/cm, our results show that the group delay can be adjusted in the range ± 2.25 fs without inducing a CEP shift. In the isochronous configuration ($d_2 = 184$ mm), when applying an electric field of 1000 V/cm (i.e. here a voltage of 500 V), the CEP shift is -5.5 rad with no induced delay. The calculated second order dispersion is kept at low level: 2.5 fs^2 for π rad CEP variation in the isochronous configuration and 0.13 fs^2 for a delay corresponding to one optical cycle in the PGD configuration. It is to be noticed that this setup does not generate any angular dispersion or spatial chirp.
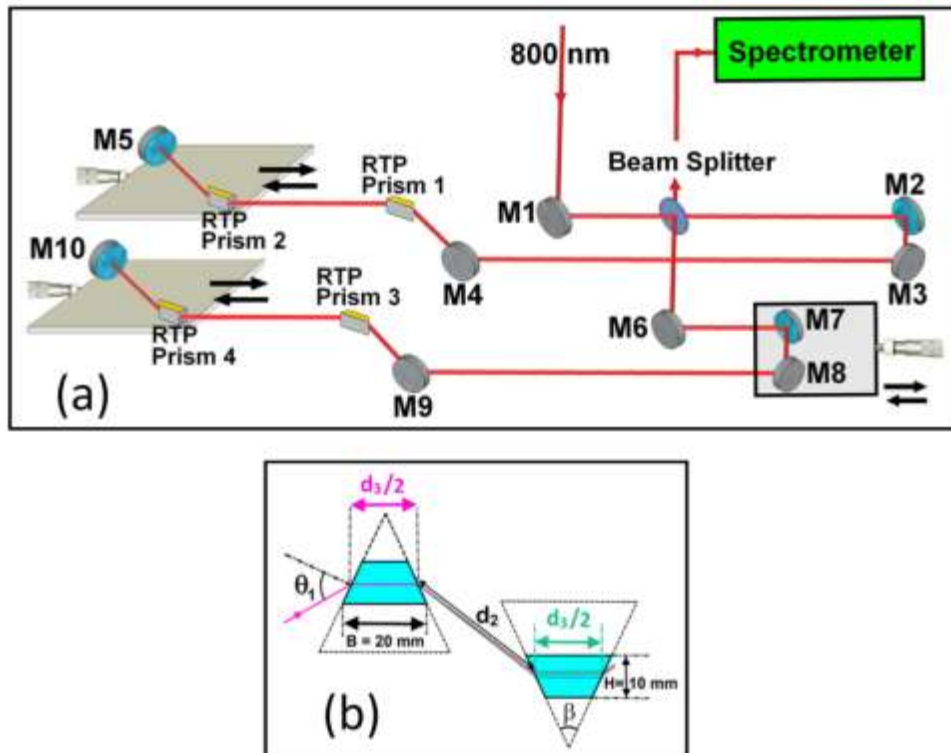

Figure 32. *Experimental set-up. (a): the 800 nm broadband (~80 nm) Ti:sapphire laser is sent in a Michelson interferometer. Each arm contains a RTP prism pair in exactly the same geometry. Only one RTP prism pair is polarized, the other arm is used to generate a reference signal. The delay is set to the chosen value with the mirrors M7/8 on a translation stage. A spectrometer with a CCD camera is used to get the fringed spectra for the different electric fields applied. (b): The two prisms are cut in such a way that the base of the isosceles trapezoid is 20 mm and the height 10 mm.*

Conclusions

Within the Eurolite project SLIC pursued studies on CEP stabilization using the Electro Optic effect in a crystal to control the CEP. By implementing a fast CEP diagnostic in the CEP

control loop, SLIC reduced the CEP remaining noise of a 20 W, 10 kHz, 25 fs TiS laser down to 320 mrad shot to shot (120 mrad when integrated over 10 shots) and to increase significantly the correction bandwidth. These achievements correspond to SLIC targets within EUROLITE.

On addition, the operation of an RTP prism pair electro-optic CEP shifter was demonstrated. Depending on the ratio d_2/d_3 between two geometrical quantities that characterize the set-up, one can make the system operate either as a "pure" CEP shifter without any group delay induced or as a "pure" delay generator without inducing a CEP shift. Even if more complex than a simple bulk RTP crystal, this arrangement also makes it possible to use lower voltages (typically 3 times lower, i.e. 90 V/rad for 5 mm aperture prisms) for a given CEP shift. Besides the clear interest of such a system to stabilize the amplified pulses from a CPA laser system seeded by a CEP stabilized oscillator via a feedback loop, it can also be used in other applications like coherent beam combination where the availability of "pure" CEP shifter and "pure" group delay generator can be a key enabling function.

⬦ References

[28]   S. Koke, C. Grebing, B. Manschwetus and G. Steinmeyer," Fast f-to-2f interferometer for a direct measurement of the carrier-envelope phase drift of ultrashort amplified laser pulses", Opt. Lett. 33, 2545 (2008).

[29]   C. Feng, J.-F. Hergott, P.-M. Paul, X. Chen, O. Tcherbakoff, M. Comte, O. Gobert, M. Reduzzi,F. Calegari,C. Manzoni,M. Nisoli,and G. Sansone, "Complete analog control of the carrier-envelope-phase of a high-power laser amplifier", Optics Express 21, 25248 (2013).

[30]   O. Gobert, P. M. Paul, J. F. Hergott, O. Tcherbakoff, F. Lepetit, P. D. Oliveira, F. Viala, and M. Comte, "Carrier-envelope phase control using linear electro-optic effect," Opt. Express 19, 5410–5418 (2011).

[31]   J.-F. Hergott, O. Tcherbakoff, P.-M. Paul, P. Demengeot, M. Perdrix, F. Lepetit, D. Garzella, D. Guillaumet, M. Comte, P. D. Oliveira, and O. Gobert, "Carrier-envelope phase stabilization of a 20 W, grating based, chirped-pulse amplified laser, using electro-optic effect in a LiNbO3 crystal," Opt. Express 19, 19935–19941 (2011).

[32]   O. Gobert, D. Rovera, G. Mennerat, M. Comte, "Linear Electro Optic Effect for High Repetition Rate Carrier Envelope Phase Control of Ultra Short Laser Pulses," Appl. Sci. 3, 168-188 (2013).

[33]   O. Gobert, N. Fedorov, O. Tcherbakoff, J.-F. Hergott, M. Perdrix, F. Lepetit, D. Guillaumet, and M. Comte, "Measurement of carrier-envelope-phase shifts using spectral interferometry with a broad frequency laser source," Opt. Commun. 285, 322–327 (2012).

[34]   O. Gobert, G. Mennerat, C. Cornaggia, D. Lupinski, M. Perdrix, D. Guillaumet, F. Lepetit, Th. Oksenhendler and M. Comte, "Electro-optic prism-pair setup for efficient high bandwidth isochronous CEP phase shift or group delay generation", submitted to Optics Communications

3.3.2 Electro-optic sampling near-infrared light (MPQ)

⬦ Objective

MPQ investigated the potential of Electro-optic sampling for direct access to near infrared electric field waveforms

⬦ Description of work

Attosecond science depends on the use of controlled laser waveforms to exploit sub-cycle light-matter interaction dynamics to translate from the femtosecond-scale of the intensity

envelope down to the attosecond domain. As a result, control over attosecond processes requires access to the exact field evolution of the laser pulse. This has primarily been done to date through the use of attosecond streaking, where an attosecond XUV pulse releases photoelectrons from a target atom or solid, which then have their momentum changed by interaction with the laser field, recording the temporal waveform in a time-delay-dependent shift in the photoelectron energy. This access to the electric field is especially important in waveform synthesis, where multiple ultrashort pulses at different carrier wavelengths are combined into a single, multi-octave transient [35]. However, attosecond streaking requires both a high laser pulse energy (for the generation of high harmonics) and an isolated attosecond pulse- the problem is that not all desired waveforms may be of the type that generates an isolated pulse, and the high energy requirement has the result that the transient is typically only measured after the interaction with a high-harmonic gas target, with inevitable nonlinear optical effects between the field synthesizer and measurement apparatus. We have pursued an alternative route to accessing the laser field that does not require the generation of an attosecond pulse: electro-optic sampling with ultrashort probe pulses.

EOS is a common technique in the terahertz spectral domain. In it, a long-wavelength, coherent pulse induces a change in the birefringence of a nonlinear crystal through the Pockels effect. A probe pulse, which fits within a half-cycle of the terahertz radiation co-propagates through the crystal with the terahertz pulse, and using a controlled time delay between the two pulses, the electric field waveform of the terahertz pulse is measured in the time domain. Extending this to the near-infrared spectral domain is difficult: the half-cycle of the radiation to be measured is as short as 2.1 fs, placing difficult requirement upon the bandwidth and phase management of the optical probe pulse. We have recently shown [36] that it is possible however, and directly measured the waveforms of near-infrared waves with wavelengths as short as 1.2 µm. The test setup and typical results are shown in Figure 9. This provides direct, time-domain access to the laser fields produced by our system, before they enter the high harmonics target, and with a dynamic range of up to 6 orders of magnitude in electric field. Unlike FROG, it provides the carrier-envelope phase directly and requires no iterative reconstruction algorithm.
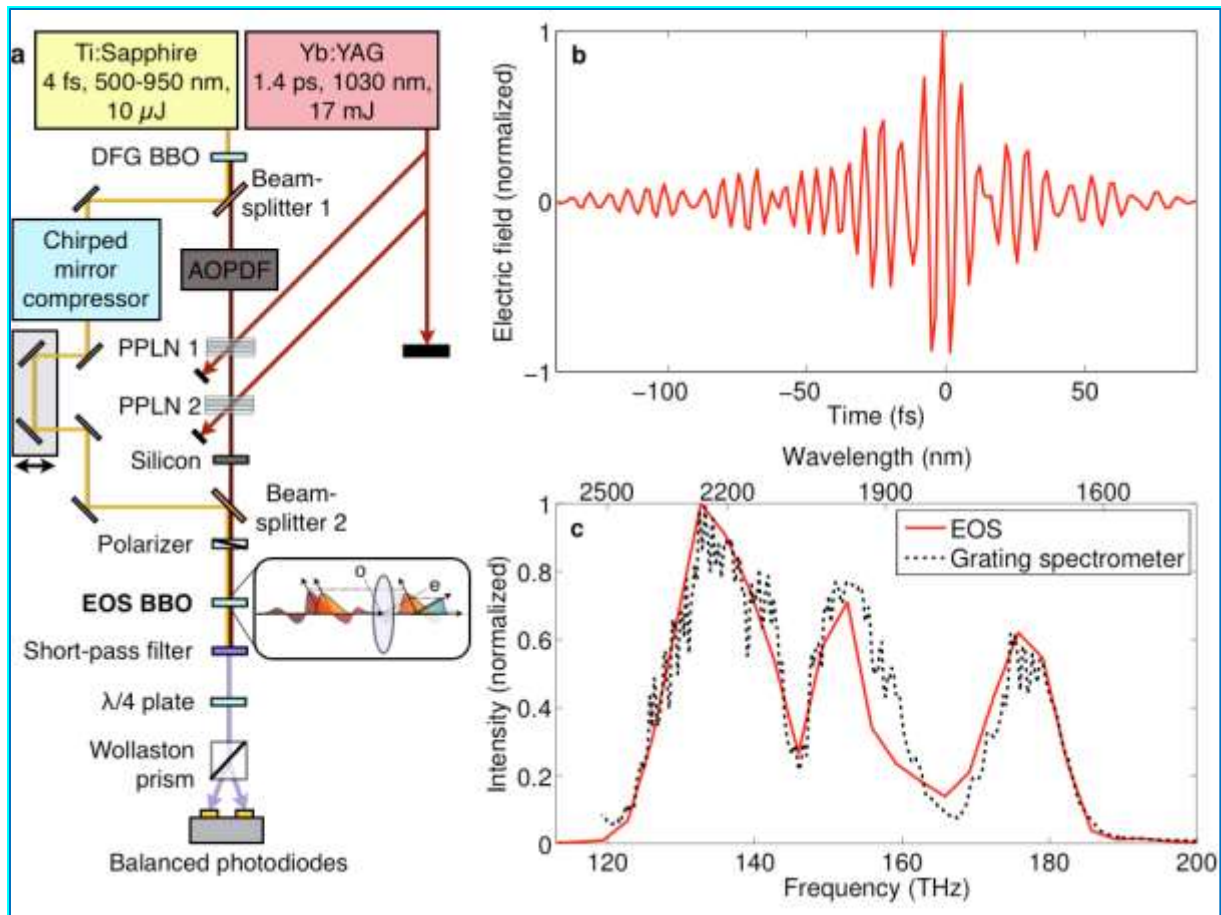
Figure 33. *Electro-optical sampling test system. (a) diagram of the system layout, AOPDF: acousto-optic programmable dispersive filter, PPLN: periodically poled lithium niobate, BBO: beta barium borate, DFG: difference frequency generation. The polarization changes induced by the infrared field on the optical probe field are measured in a balanced detection scheme, allowing for high dynamic range. (b) Electric field measured via EOS, exhibiting a FWHM intensity duration of 11 fs. (c) Spectrum obtained by FFT of the temporal field compared with that measured with a conventional (calibrated), grating-based spectrometer with extended InGaAs detection elements (Ocean Optics NIRQuest 512). Source: [36]*

✦ Conclusion

MPQ demonstrated extension of the electro-optic sampling (EOS) technique to the near infrared, allowing for direct access to near infrared electric field waveforms.

✦ References

[35] [1] A. Wirth, et al. "Synthesized light transients," Science 334, 195 2011.

[36] [2] S. Keiber, S. Sederberg, A. Schwarz, M. Trubetskov, V. Pervak, F. Krausz, and N. Karpowicz, "Electro-optic sampling of near-infrared waveforms," submitted

3.3.3 Real-Time, Single-Shot, Carrier-Envelope-Phase Measurement of a Multi-TeraWatt Laser [37]

✦ **Objective**

HIJ sought at performing single shot characterisation of the CEP of a Multi-TeraWatt Laser using an ATI phase meter.

✦ **Description of work**

The investigation of CEP effects in experiments, e.g. surface high harmonic generation, at high power laser systems requires a characterization setup witch can be operated with low repetition rates. Usual feedback loops which are used to stabilize the CEP are not applicable under these conditions.

HIJ performed a single-shot CEP measurement of the 40 TW laser system "Jeti" at 1Hz repetition rate with an ATI phasemeter [37]. By compressing a tiny fraction of the 25fs pulses with a hollow core fibre, chirped mirror setup to 4fs, it was possible to measure the CE-phase with an uncertainty of 164mrad for 86% of the shots. For the remaining 14% laser instabilities resulted in an insufficient electron signal for CEP evaluation. Since there is a fixed CE-phase relation between the measured and the main pulse of the laser system, by taking into account the phase energy coupling in the hollow core fibre, one can use the measured phase for phase tagging experiments with the main beam.
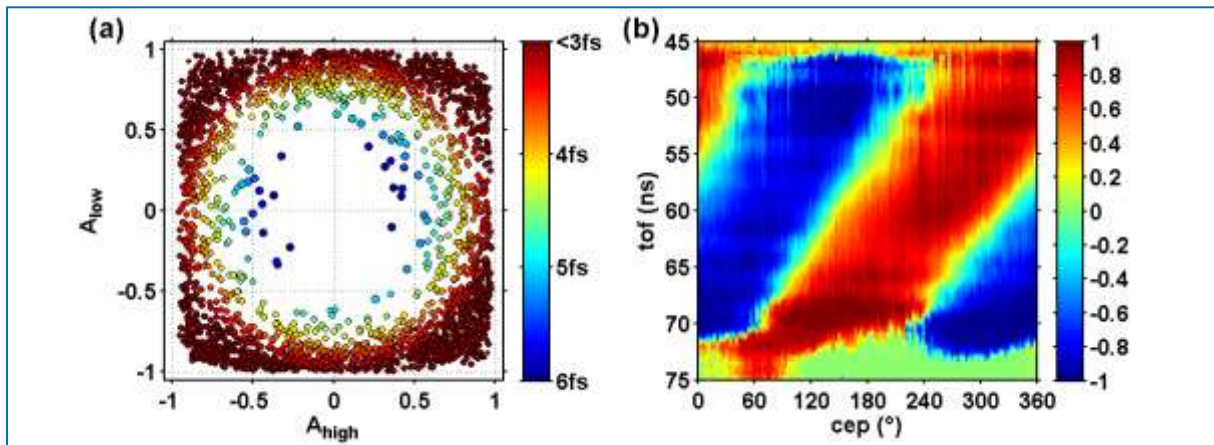

Figure 34. *(a) parametric asymmetry plot for 86% of 3500 consecutive shots (b) CEP tagged asymmetry of the left- right electron spectra*

Momentum resolved study of the saturation intensity in multiple ionization [38]

Strong-field ionization of atoms is of fundamental interest for many phenomena like laser-based electron or ion acceleration by ultra-intense laser pulses. When atoms are exposed to super-intensive or relativistic laser intensities, they will be ionized to high charge states. In the optical regime, the ionization probability depends highly nonlinear on the field strength.

An accurate knowledge of the ionization dynamics over a large range of charge states plays an important role in strong-field laser physics and plasma physics.

HIJ carried out a momentum resolved study of strong field multiple ionization of ionic targets. A beam of Ne^+ ions is ionized up to charge state 5 by an elliptically polarized laser field with peak intensities of up to about 10^{17} W/cm^2 and the full 3D momentum of the ionized particles is measured. In order to quantify the observations and to subsequently enable the

determination of photoelectrons' momenta for each ionization step, a method to deconvolve the measured momentum distribution of multiply ionized ions was developed. This technique allows to reconstruct the electron momenta from the ion momentum distributions after multiple ionization up to four sequential ionization steps and to extract the saturation intensities as well as of the electron release times during the laser pulse.
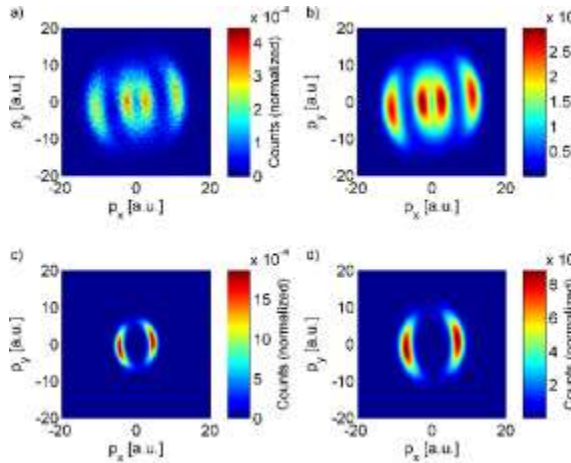

Figure 35. *a) Measured ion distribution of Ne3+, b) Simulated momentum distribution for Double ionization from fit method, Simulated momentum distribution for first (c) and second (d) single ionization from fit method*
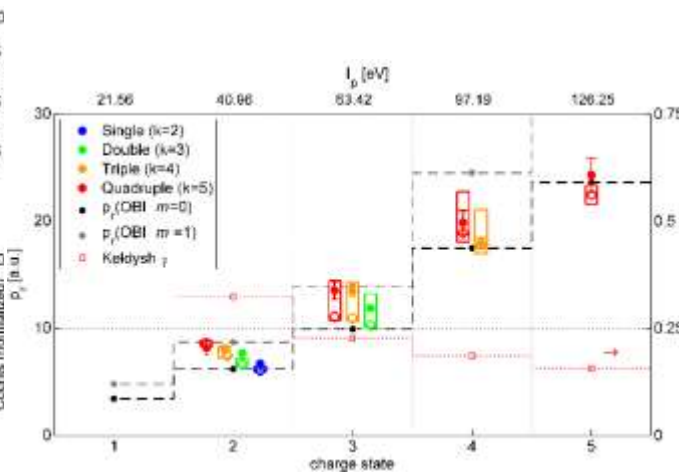
Figure 36. *Comparison of the measured final momentum (solid circles) with results of calculations of the ionization rate (open circles and rectangles). The red open squares (right scale) represent the trend of Keldysh parameter.*

Thus, the typically large experimental uncertainties in the intensity determination are removed. This allows the retrieval of averaged ionization times of all charge states created in the laser focus. The measured results are compared with predictions of frequently used models of strong field ionization in the quasistatic tunneling and over-the-barrier regime.

⬥ Conclusion

Using an ATI phase meter, HIJ succeeded to carry out single shot measurement of the CEP of a multi-TW laser system. It will be extremely useful for future surface high harmonic experiments to investigate their CEP dependence.

⬥ References

[37]   Rathje, T. et al., Review of attosecond resolved measurement and control via carrier-envelope phase tagging with above-threshold ionization, 2012 J. Phys. B: At. Mol. Opt. Phys. 45 074003

[38]   Wustelt, M., et al., Momentum-resolved study of the saturation intensity in multiple ionization. Phys. Rev. A 91, 031401. DOI: 10.1103/PhysRevA.91.031401 [no open access]

3.4   Extending the frequency-comb advantages to the Mid-IR

3.4.1   Development of Mid-IR frequency-comb based laser sources at LENS

⬥ Development of a comb-referenced Mid-IR quantum cascade laser

LENS achieved the linewidth narrowing of a room-temperature mid-infrared quantum cascade laser by phase-locking to a difference-frequency-generated radiation referenced to an optical frequency comb synthesizer [39, 40].

LENS used a distributed-feedback QCL emitting at 4.3 um operated at a temperature of 283K and a current of 710 mA, delivering an output power of about 5 mW. The radiation to which the QCL has been locked to is produced by non-linear DFG process in a periodically-poled LiNbO3 crystal by mixing an Yb-fiber-amplified Nd:YAG laser at 1064 nm and an external-cavity diode laser (ECDL) emitting at 854 nm. The peculiar locking scheme, employing a direct-digital-synthesis (DDS) technique, makes the ECDL to be effectively phase-locked to the Nd:YAG laser, while the OFCS just behaves as a transfer oscillator adding negligible phase-noise to the DFG radiation. As a consequence, the mid-IR radiation is referenced to the Cs frequency standard through the OFCS, but its linewidth is independent from that of the OFCS. A schematic of the experimental setup is shown in Figure 37.
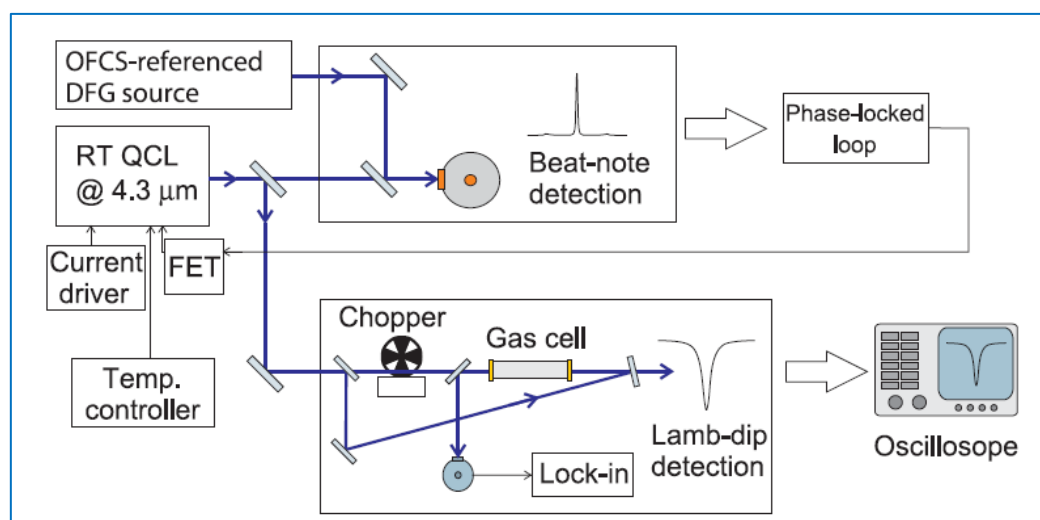

Figure 37. Schematic of the experimental setup. There are two main parts: the beat-note detection between the QCL and DFG for the phase-locking and the detection of the SA spectroscopy signal for the absolute frequency measurement of the CO2 transitions.

A small portion of the QCL beam, extracted by a beam-splitter, is used for the phase-lock: It is overlapped to the DFG source through a second beam splitter and sent to a 200-MHz-bandwidth HgCdTe detector. A 100-MHz beatnote is detected by using few uW of both QCL and DFG sources. The beat-note is processed by a home-made phase detection electronics, which compares it with a 100-MHz local oscillator and provides the error signal for closing the phase-locked loop. A home-made proportional-integral-derivative (PID) electronics process the error signal and send it to the gate of a field effect transistor (FET) to fast control the QCL driving current.

The main portion of the QCL radiation is used for frequency-noise characterization and for spectroscopy. We demonstrated the phase-locking with a 250-kHz bandwidth and a residual rms phase-noise of 0.56 rad, leading to a subkilohertz-linewidth QCL radiation. The QCL frequency stability is 6×10^{-13} in 1 s with an absolute traceability accurate in 2×10^{-12}, both limited by the Rb-GPS-disciplined 10-MHz quartz oscillator reference of the OFCS [39].

In order to test the spectral performances of the phase-locked QCL in terms of resolution, we performed saturated absorption (SA) sub-Doppler spectroscopy of the CO2 molecule around 4.3 um in a single-pass cell. The SA setup, depicted schematically in Fig. 37, uses about 5 mW of power of the QCL in a standard pump-probe configuration. Thanks to the absolute reference, it is possible to measure the absolute center frequency of several molecular

transition of the $(01^11 - 01^10)$ ro-vibrational band of CO2. In the SA scheme, the Lamb dip at the center of the Doppler-broadened molecular line is detected (Fig. 37). An optical chopper on the pump beam, combined with lock-in detection, allows to automatically cancel out the Doppler background and to retrieve the Lorentzian Lamb dip profile with an increased signal-to-noise ratio. The frequency of the phase-locked QCL is scanned across the Lamb dip by tuning the frequency of the DFG source. The link to the OFCS automatically provides each scan with the absolute frequency scale.

The achieved relative uncertainties range from 1×10^{-11} to 5×10^{-11}, improving by three to four orders of magnitude the previous tabulated values for such frequencies. Moreover, thanks to this precision level, self-pressure-shift coefficients due to collisional processes of CO2 molecules are reported for the first time [40].

⊹ Optical radiocarbon dioxide concentration measurements

By exploiting the unique features of a highly performing mid-IR coherent light source, combined with the strong molecular absorption of carbon dioxide in the mid-IR, LENS succeeded in measuring, for the first time, the spectral area (and hence the absolute radiocarbon dioxide [$^{14}C^{16}O_2$] concentration) of the $(00^01–00^00)$ P(20) line of the $^{14}C^{16}O_2$ isotopologue [41].

A newly developed laser spectroscopy technique allowed us to achieve the extreme sensitivity necessary to detect the $^{14}C^{16}O_2$ molecules at their tiny natural abundance with an all-optical setup that is much more compact and less expensive than accelerator mass spectrometry (AMS). The new spectroscopic technique, named SCAR (saturated- absorption cavity ring-down) makes use of saturation of molecular absorption to enhance resolution (up to 3 orders of magnitude) and sensitivity (~20 times) with respect to conventional cavity ring-down spectroscopy. The SCAR working principle has been deeply described in [42], and can be shortly described as follows. An optical cavity filled with CO_2 is illuminated with an intense CW laser tuned to excite the targeted $(00^01–00^00)$ P(20) ro-vibrational transition of $^{14}C^{16}O_2$. The specific resonance line was selected following dual criteria: maximum absorption coefficient and minimum level of interferences from all other nearby lines. When the laser is turned off, photons stored in the cavity decay due to both $^{14}C^{16}O_2$ absorption and mirror leakage. Because light intensity saturates the absorption of the $^{14}C^{16}O_2$ molecule, the initial decay characteristic is affected by losses from the mirrors only. Once this background is subtracted, we can determine the absolute quantity of $^{14}C^{16}O_2$ from the linear molecular absorption encoded in the decay tail.

Combining SCAR with a frequency-comb-linked difference-frequency-generated (DFG) coherent source, delivering up to 30 mW continuous-wave (CW) radiation tunable around 4.5-um wavelength, allowed us to set an unprecedented limit in trace gas detection, accessing the part-per-quadrillion (ppq, 10^{-15}) concentration range. SCAR-based results are still 1 order of magnitude below those of AMS, but this technique has ample room for improvement. Finally, the SCAR dynamic range encompasses more than 5 orders of magnitude in measurable concentration values. This range is much wider than in AMS setups, which are typically limited to 3 orders of magnitude, even when designed for pharmaceutical applications.

The simplified schematics of the experimental apparatus are shown in Figure 38.
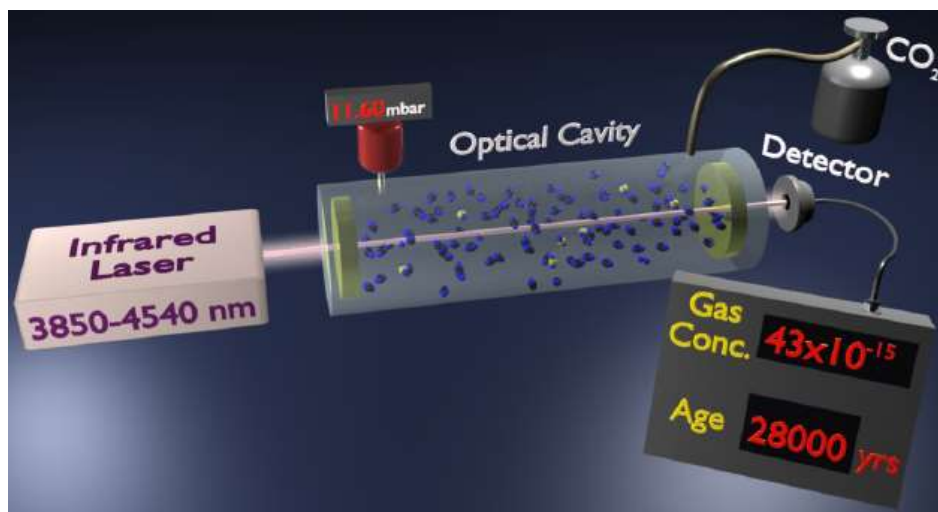
Figure 38. Schematic of the experimental setup for SCAR detection of natural abundance $^{14}C^{16}O_2$.

High coherence frequency comb around 4330 nm

LENS succeeded in the generation of a frequency comb around 4330 nm with an unprecedented coherence of the single teeth [43].

Generating the comb within a Ti:sapphire laser cavity by a difference-frequency process and using a phase-lock scheme based on direct digital synthesis, we achieved a tooth linewidth of 2.0 kHz in a 1-s timescale (750 Hz in 20 ms). The generated per-tooth power of 1 µW ranks this comb among the best ever realized in the mid-infrared in terms of power spectral density.

In Fig. 36 we show the experimental setup, based on a mode-locked Ti:Sa laser with a repetition rate of about 1 GHz, spectrally broadened to one octave operation range (500–1100 nm) by a photonic crystal fiber (NIR-comb). The oscillator controlling the repetition frequency is referenced to a Rb/GPS-disciplined 10-MHz quartz clock with a stability of 6×10^{-13} at 1 s and an accuracy of 2×10^{-12}. The portion of the NIR-comb spectrum above 1 µm wavelength is selected by a dichroic mirror and sent to an Yb3+ fiber amplifier: the output radiation, whose spectrum is limited by the amplifier gain bandwidth, is injected into the Ti:Sa laser cavity by another dichroic mirror. The amplifier output is used as signal in a MgO:PPLN multiperiod crystal to generate idler radiation (MIR-comb), where the pump is the intracavity Ti:Sa radiation. The MIR-comb radiation is extracted from the cavity taking advantage of different refraction angles at the facet of the crystal, cut at Brewster angle for the pump. The Ti:Sa laser is optically injected by an external-cavity diode laser (ECDL) in order to make it unidirectional and single frequency.
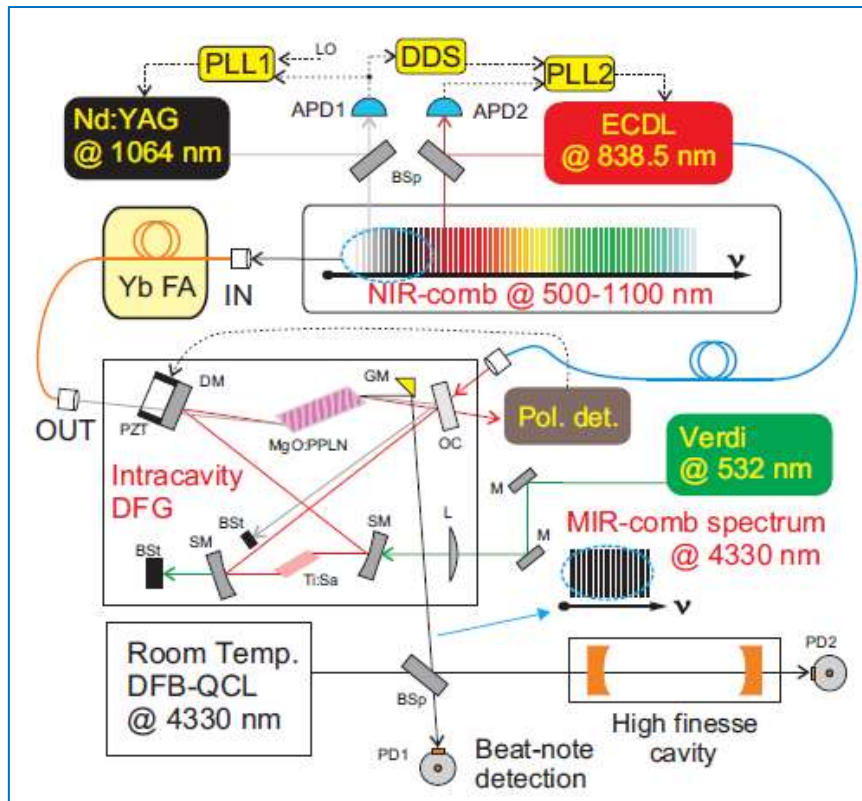
Figure 39. *Experimental setup for the generation of a Mid-IR comb.*

In order to estimate the coherence of the MIR-comb we used a high-finesse cavity as frequency-to-amplitude converter. The generated spectrum spans 27 nm, with a center wavelength tunable from 4.2 to 5.0 μm.

The Mid-IR comb was then used as an accurate and highly stable frequency reference at 4330 nm. By phase locking a DFB quantum cascade laser to one of the comb teeth this resulted in a powerful and narrow-linewidth source enabling high-precision spectroscopy in the Mid-IR.
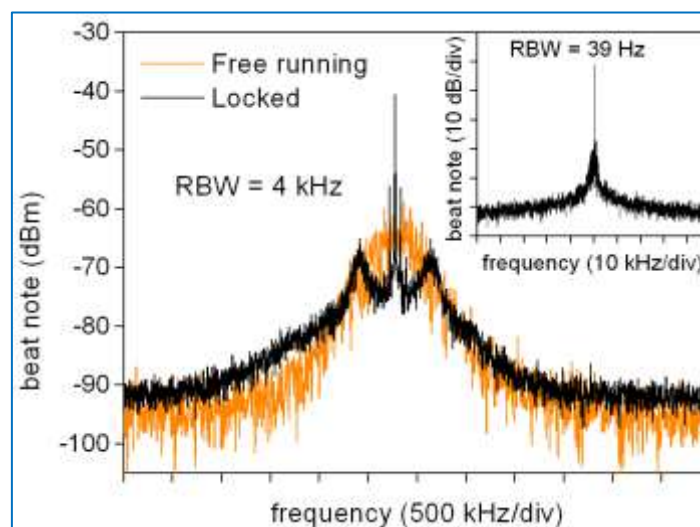

Figure 40. *Beat-note between the QCL and one MIR OFC tooth, in free-running and phase-locked-conditions.*

Moreover, the Mid-IR frequency-comb itself was directly used for broadband direct comb spectroscopy, showing the possibility of absolute frequency measurements with wide tunability (4.2 - 5.0 µm) and high coherence (2.0 kHz linewidth).
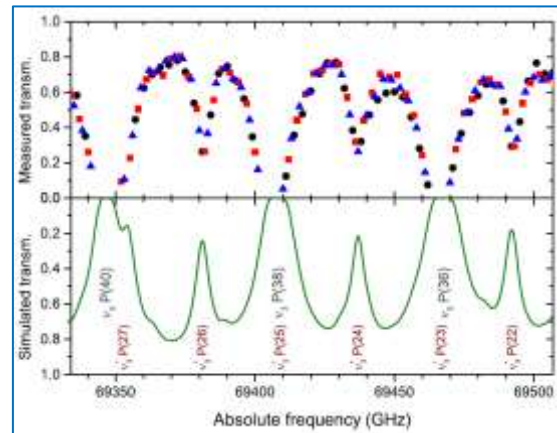

Figure41. *MIR OFC air transmission spectrum measured with the Vernier technique.*

Vernier spectroscopy of CO_2 absorption in ambient air was demonstrated with individually-resolved comb teeth [44].

Mid-IR intracavity quartz-enhanced photoacoustic spectroscopy

LENS developed a new spectroscopic technique, named intracavity quartz-enhanced photoacoustic spectroscopy (I-QEPAS), and employed it for sensitive trace-gas detection in the mid-IR [46].

It relies on a distributed-feedback QCL emitting at 4.33 µm and is based on a combination of photoacoustic spectroscopy with a build-up optical cavity. This new technique merges the advantages of QEPAS with those of cavity-enhanced absorption spectroscopy. It uses a compact, robust, and cost-effective sensor and the same detection module for all spectral ranges and gas samples; it presents zero-background detection and a linear response with sample concentration. The combination with the enhancement cavity allowed us to improve sensitivity by a factor of 250 with respect to standard QEPAS.
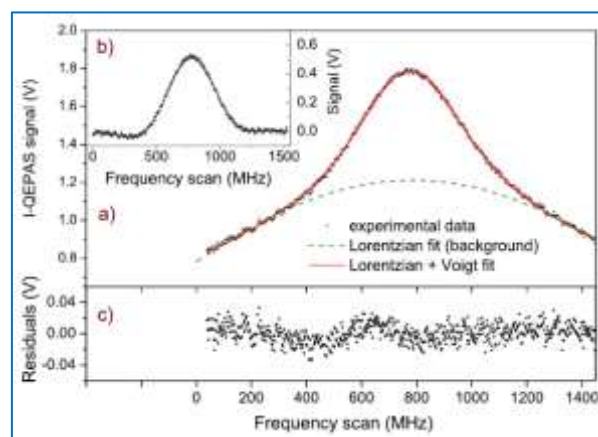

Figure 42. *I-QEPAS spectral scan of a 50 ppb CO2:N2 gas sample.*

✚ Conclusions

The LENS group actively phase-locked a quantum cascade laser to a difference-frequency-generated (DFG) non-linear source referenced to a near-IR optical frequency comb, achieving a subkilohertz linewidth and a Cs-traceable mid-IR source delivering tens of mW. This novel source has been used for sub-Doppler spectroscopy of CO2 transitions at 4.3 um, performing absolute frequency measurements of several lines with few kHz uncertainties.

The possibility of realizing comb-referenced Mid-IR sources with high power and narrow linewidths, combined with novel spectroscopic techniques for high sensitivity, allowed LENS to perform optical radiocarbon dioxide concentration measurements at unprecedented levels.

On addition, a Mid-IR frequency comb was demonstrated with more than 400 GHz span, 1 GHz rep. rate and subkilohertz-linewidth teeth, by an intra-cavity DFG process in a Ti:sapphire laser. The Mid-IR comb was used for frequency-referencing a DFB quantum cascade laser and for direct frequency-comb spectroscopy in the Mid-IR.

Finally, a new spectroscopic technique, merging the advantages of intracavity absorption and photoacoustic spectroscopy has been developed for improved sensitivity in the Mid-IR.

✚ References/Publications

[39] Comb-assisted subkilohertz linewidth quantum cascade laser for high-precision mid-infrared spectroscopy, I. Galli, M. Siciliani de Cumis, F. Cappelli, S. Bartalini, D. Mazzotti, S. Borri, A. Montori, N. Akikusa, M. Yamanishi, G. Giusfredi, P. Cancio, and P. De Natale, Applied Physics Letters 102, 121117 (2013). http://dx.doi.org/10.1063/1.4799284

[40] Absolute frequency measurements of CO2 transitions at 4.3 µm with a comb-referenced quantum cascade laser, I. Galli, S. Bartalini, P. Cancio, F. Cappelli, G. Giusfredi, D. Mazzotti, N. Akikusa, M. Yamanishi, and P. De Natale, Molecular Physics 111, 2041-2045 (2013). DOI: 10.1080/00268976.2013.782436

[41] Optical detection of radiocarbon dioxide: first results and AMS intercomparison.I. Galli, S. Bartalini, P. Cancio, P. De Natale, D. Mazzotti, G. Giusfredi, M. E. Fedi, and P. A. Mandò, Radiocarbon 55, 213-223 (2013). DOI: 10.2458/azu_js_rc.55.16189

[42] Theory of saturated-absorption cavity ring-down: radiocarbon dioxide detection, a case study, G. Giusfredi, I. Galli, D. Mazzotti, P. Cancio, and P. De Natale, J. Opt. Soc. Am. B 32(10), 2223 (2015) DOI: 10.1364/JOSAB.32.002223

[43] High-coherence mid-infrared frequency comb I. Galli, F. Cappelli, P. Cancio, G. Giusfredi, D. Mazzotti, S. Bartalini, and P. De Natale, Optics Express (2013), 21, 28877 (2013). DOI:10.1364/OE.21.028877

[44] Mid-infrared frequency comb for broadband high precision and sensitivity molecular spectroscopy I. Galli, S. Bartalini, P. Cancio, F. Cappelli, G. Giusfredi, D. Mazzotti, N. Akikusa, M. Yamanishi, and P. De Natale, Opt. Lett. 39, 5050 (2014) DOI: 10.1364/OL.39.005050

[45] Intracavity quartz-enhanced photoacoustic sensor. S. Borri, P. Patimisco, I. Galli, D. Mazzotti, G. Giusfredi, N. Akikusa, M. Yamanishi, G. Scamarcio, P. De Natale, and V. Spagnolo, Appl. Phys. Lett. 104, 091114 (2014) DOI: 10.1063/1.4867268

4   Conclusion

The work carried out by the LASERLAB partners involved in the objective 3 of EUROLITE lead to significant achievements that constitute important steps towards the routine production of energetic attosecond XUV pulses and their application in pump probe experiments with sub-femtosecond resolution.

First, the development of lasers drivers for attosecond pulse generation has been continued using several complementary approaches. Using a Titanium-Sapphire laser associated with an innovative post-compression scheme, LOA was able to produce sub-4 fs pulses at 800 nm with peak power close to the Terawatt level. Mid–IR sources were implemented at ICFO and MPQ. Based on Optical Parametric Amplification, ICFO's set-up generates sub-2-cycle pulses at 1850 nm that were used to produce broadband soft X-ray radiation in the entire water window for life science applications. Significant progress were also made on the MPQ laser based on high energy OPCPA (Optical Chirped Pulse Parametric Amplification) at 2,1 µm to the point where the system is now being used for exciting new experiments on light-wave driven dynamics probed by high-energy attosecond pulses. CELIA implemented a very high repetition rate (100 kHz) laser based on Fiber Chirped Pulse Amplification. Thanks to significant improvements in terms of stability and reliability, generating harmonics up to H29 was made possible and XUV light with up to $4x10^{10}$ photons per second has been collected on the detector. CELIA also demonstrated post-compression of multi-Terawatt pulses for the generation of energetic attosecond pulses.

In addition, advanced set-ups and optimized configurations were tested to improve the generation of femto/atto XUV pulses through High Harmonic Generation. HIJ optimised surface harmonics generation by adjusting the laser contrast and also through the use of structured targets. Interferometric pulse gating, that is also a promising route to get energetic attosecond pulses from multi-cycle intense lasers, has been used at HIJ and FORTH. HIJ demonstrated polarisation gating on a 40TW laser while FORTH was able to generate energetic XUV super-continua for two-XUV-photon processes with 1 fs scale temporal resolution. This achievement allowed to carry out the first ever XUV-pump-XUV-probe studies of 1fs scale dynamics.

CEP stabilisation and measurement is also central to controlled single attosecond pulse generation. SLIC pursued studies on CEP stabilization using Electro Optic phase shifters to get increased correction bandwidth and isochronous stabilisation. MPQ extended the electro-optic sampling (EOS) technique to the near infrared to get direct access to the electric field waveforms. Single-shot CEP measurements of a 40 TW laser at 1Hz were made at HIJ using the home developed ATI phasemeter.

Finally, LENS succeeded in developing advanced laser set-ups in the mid-IR for applications including ultra-sensitive detection and monitoring of molecules of atmospheric and astrophysical interest.

5   Publications resulting from this work (with Laserlab acknowledgement)

– "Carrier-envelope-phase-stable 1.2 mJ, 1.5 cycle laser pulses at 2.1 µm," Y. Deng et al., Optics Letters **37**, 4973 (2013). doi: 10.1364/OL.37

– "Decoupling chaotic amplification and nonlinear phase in high-energy thin-disk amplifiers for stable OPCPA pumping," H. Fattahi et al., Opt. Express **22**, 31440 (2014). doi: 10.1364/OE.22.031440
   [open access]

– "Electro-optic sampling of near-infrared waveforms" S. Keiber et al., submitted

- **"Post-compression of high energy terawatt-level femtosecond pulses and application to high order harmonic generation"**, O. Hort et al., J. Opt. Soc. Am. B **32**, 1055 (2015). doi: 10.1364/JOSAB.32.001055dx.

- "Spatio–spectral structures in high-order harmonic beams generated with Terawatt 10-fs pulses", A. Dubrouil et al., Nature Communication **5**:4637 (2014). doi:10.1038/ncomms5637

- "Numerical evaluation of ultrabroadband parametric amplification in YCOB", H. Pires et al., JOSAB **31**, 2608-2614 (2014). doi: 10.1364/JOSAB.31.002608

- "Importance of intensity-to-phase coupling for water-window high-order-harmonic generation with few-cycle pulses", S. M. Teichmann et al., Phys. Rev. A **91**, 063817 (2015). doi: 10.1103/PhysRevA.91.063817

- "Spatiotemporal isolation of attosecond soft X-ray pulses in the water window", F. Silva et al., Nature Commun. **6**, 6611 (2015). doi: 10.1038/ncomms7611 *[open access]*

- "Compression of CEP-stable multi-mJ laser pulses down to 4 fs in long hollow fibers", F. Böhle et al., Laser Phys. Lett. **11**, 095401 (2014). doi: 10.1088/1612-2011/11/9/095401

- "Harmonic generation from relativistic plasma surfaces in ultrasteep plasma density gradients", C. Rödel, et al., Physical Review Letters, 2012. 109(12): p.125002. doi: 10.1103/PhysRevLett.109.125002

- "Sensitivity calibration of an imaging extreme ultraviolet spectrometer-detector system for determining the efficiency of broadband extreme ultraviolet sources", S. Fuchs et al., Review of Scientific Instruments, 2013. **84**(023101). doi: 10.1063/1.4788732

- "Generation of 10 μW relativistic surface high-harmonic radiation at a repetition rate of 10 Hz", J. Bierbach et al., New Journal of Physics, 2012. **14**. doi: 10.1088/1367-2630/14/6/065005 [*open access]*

- "Near-monochromatic high-harmonic radiation from relativistic laser-plasma interactions with blazed grating surfaces", M. Yeung et al., New Journal of Physics, 2013. **15**(025042). doi: 10.1088/1367-2630/15/2/025042 [open access]

- "Broadband XUV polarimetry of high harmonics from plasma surfaces using multiple Fresnel reflections", T. Hahn et al., Applied Physics B, 2015. Volume 118, Issue 2, pp 241-245. doi: 10.1007/s00340-014-5977-9

- "Single-shot autocorrelator for extreme-ultraviolet radiation" G. Kolliopoulos et al., J. Opt. Soc. Am. B **31** 926-938 (2014) doi: 10.1364/JOSAB.31.000926

- "Unravelling the quantum optical underpinnings of high-order harmonic generation" K. Kominis et al., Phys. Rev. A**89**, 063827 (2014). doi: 10.1103/PhysRevA.89.063827

- "Revealing quantum path details in high-field physics" G. Kolliopoulos et al., Phys. Rev. A**90**, 013822 (2014). doi: 10.1103/PhysRevA.90.013822

- "Electro-optic prism-pair setup for efficient high bandwidth isochronous CEP phase shift or group delay generation", O. Gobert et al., submitted to Optics Communications

- "Theory of saturated-absorption cavity ring-down: radiocarbon dioxide detection, a case study", G. Giusfredi et al., J. Opt. Soc. Am. B **32**(10), 2223 (2015) doi: 10.1364/JOSAB.32.002223

- "Intracavity quartz-enhanced photoacoustic sensor", S. Borri et al., Appl. Phys. Lett. **104**, 091114 (2014) doi: 10.1063/1.4867268

- "Mid-infrared frequency comb for broadband high precision and sensitivity molecular spectroscopy", I. Galli et al., Opt. Lett. **39**, 5050 (2014). doi: 10.1364/OL.39.005050